NATIONAL ADVISORY COMMITTEE FOR AERONAUTICS

TECHNICAL NOTE 3433

TOTAL LIFT AND PITCHING MOMENT ON THIN ARROWHEAD WINGS OSCILLATING IN SUPERSONIC POTENTIAL FLOW

By H. J. Cunningham

Langley Aeronautical Laboratory
Langley Field, Va.

Washington
May 1955

NATIONAL ADVISORY COMMITTEE FOR AERONAUTICS

TECHNICAL NOTE 3433

TOTAL LIFT AND PITCHING MOMENT ON THIN ARROWHEAD WINGS OSCILLATING IN SUPERSONIC POTENTIAL FLOW

By H. J. Cunningham

SUMMARY

Expressions based on linearized supersonic potential theory are given for the total lift and moment coefficients of thin arrowhead wings oscillating in pitch and vertical translation. The arrowhead plan form as treated herein includes all pointed-tip wings; the delta plan form with an unswept trailing edge is a special case. A restriction is that the component of flow normal to the trailing edge must be supersonic or sonic. The total coefficients have been obtained by integration of the section coefficients given in NACA Report 1099 for the subsonic-leading-edge wing (to the fifth power of the frequency) and in NACA Technical Note 2494 for the supersonic-leading-edge wing (to the third power of the frequency). The accuracy of these expressions extends to sufficiently high frequencies to make them potentially useful in flutter applications.

A correlation of coefficient notation is given for the present flutter coefficients, for dynamic stability coefficients, and for the exact flutter coefficients developed by Miles for the supersonic-leading-edge delta plan form. For the supersonic-leading-edge delta wing, curves are given to show the comparison of these three types of coefficients. The relative importance of higher order frequency terms as compared with the lowest order frequency term in each flutter coefficient decreases rather rapidly with the following parametric changes: increasing Mach number, increasing leading-edge sweep angle (except for the supersonic-leading-edge delta wing), and decreasing trailing-edge sweep angle. These parametric changes have the concurrent result that the accuracy of the approximate coefficients increases for any given reduced frequency.

Sweeping the trailing edge back has, in general, an unfavorable or destabilizing effect on the damping of pitching oscillations. An unstable damping in pitch, however, does not necessarily imply an instability of the wing if the wing is also free to translate vertically. For these two degrees of freedom, examples are given of requirements on mass ratio and pitching radius of gyration for the condition of no elastic restraint, that is, with the wing in free flight.

INTRODUCTION

The present paper is concerned with the integrated or total aerodynamic forces and pitching moments on thin oscillating arrowhead wings in linearized supersonic potential flow. The class of wing plan form treated includes all arrowhead wings with subsonic or supersonic sweptback leading edges and supersonic sweptback or sweptforward trailing edges meeting at pointed tips. The delta wing with an unswept trailing edge is a special case.

The total forces and pitching moments on these arrowhead plan forms can be useful in several applications including the following: dynamic stability analysis of tailless arrowhead-wing configurations extending to very-short-period oscillations, flutter analysis of arrowhead wings or tails involving rigid-body components of motion, analysis of the oscillations of a system consisting of a rigid wing or tail mounted on a flexible fuselage, and analysis of oscillations of a rigid all-movable control surface which either has a full-span arrowhead plan form or is a half-span surface mounted on a body which acts as a reflection plane.

References 1 and 2 give expressions for total lift and moment on rigid delta plan forms with all edges supersonic, and these expressions apply to all frequencies of oscillation. Expressions for section lift and moment of the more general arrowhead plan form are given in reference 3 for subsonic leading edges and in reference 4 for supersonic leading edges. The expressions of references 3 and 4 were developed on the basis of an expansion of the velocity potential as a power series in the frequency of oscillation and retention of the first few terms in the series. Reference 3 retains the fifth power of the frequency and reference 4 retains the third power. The total forces and moments of the present paper are the spanwise integrals of the expressions for the section forces and moments of references 3 and 4.

References 5 to 8 give various longitudinal static and dynamic stability coefficients for the arrowhead plan form based on the retention of terms for only the zero and first powers of the frequency of oscillation. Reference 5 deals with the subsonic-leading-edge arrowhead wing, and references 6, 7, and 8 deal with the supersonic-leading-edge arrowhead wing, as well as a more general plan form with a taper ratio greater than zero.

Because of some confusion which exists with regard to the relation of flutter and stability coefficients, a correlation is presented herein of the notation of the flutter coefficients of the present paper, the exact flutter coefficients of reference 1, and the dynamic stability coefficients as given in reference 5. Furthermore, in order to permit assessment of the accuracy of the first-order frequency coefficients of

references 5 to 8 and of the higher order frequency coefficients of the present paper in comparison with the exact coefficients of references 1 and 2, examples of these three types of coefficients are given in the form of curves as functions of the frequency parameter $\bar{\omega}$ for sonic- and supersonic-leading-edge delta wings.

SYMBOLS

A_i, P_j, Q_j, R_j — constants depending on βC, expressed and tabulated in reference 3; $i = 0, 1, 2,$ and 3 and $j = 1, 2, \ldots 20$

b — semichord of wing at root or at midspan

$\bar{c}$ — mean aerodynamic chord

$C = \cot \Lambda = \tan \epsilon$

C_{L_α}', $C_{L_{\dot{\alpha}}}'$, C_{L_q}', C_{m_α}', $C_{m_{\dot{\alpha}}}'$, C_{m_q}' — longitudinal stability coefficients referred to stability axes, defined in reference 5

$D = \tan \Lambda_{TE}$

E_{mn}, F_{mn}^{e}, G_{mn}, H_{mn}^{e} — section functions of β, ν, and trailing-edge coordinate, defined in reference 4

$\bar{E}_{mn}$, $\bar{F}_{mn}^{e}$, $\bar{G}_{mn}$, $\bar{H}_{mn}^{e}$ — spanwise integrals of E_{mn}, F_{mn}^{e}, G_{mn}, and H_{mn}^{e}, given by equations (A12), (A17), (A23), and (A24), respectively

h — vertical displacement of axis of rotation, positive downward, $h_0 e^{i\omega t}$

$\dot{h} = \partial h / \partial t$

h_0 — amplitude of vertical displacement of axis of rotation

$I_{1,m}$, $I_{2,n}^{m}$, $I_{3,n}$, $I_{3,n}'$, $I_{4,n}$, $I_{4,n}'$ — spanwise integrals defined by equations (A1) to (A11) and (A18) to (A22)

k — reduced frequency, $b\omega/V$

$K_{1,n}'$, $K_{1,n}''$, $K_{2,n}'$, $K_{2,n}''$ — spanwise integrals defined by equations (A14) to (A16)

L_i, M_i — components of section lift and moment coefficients for a pitch and moment axis at μ_0, appearing in equations (1) and (2)

$L_1 + iL_2$ — complex lift coefficient due to vertical translation, positive L_1 indicates lift acts upward for positive h (lift opposes h) and positive L_2 indicates lift acts upward for positive $\dot{h}$ (lift opposes or damps $\dot{h}$)

$L_3 + iL_4$ — complex lift coefficient due to pitching oscillation, positive L_3 indicates lift acts upward for positive α and positive L_4 indicates lift acts upward for positive $\dot{\alpha}$

$M_1 + iM_2$ — complex moment coefficient due to vertical translation, positive M_1 indicates moment acts leading edge down for positive h and positive M_2 indicates moment acts leading edge down for positive $\dot{h}$

$M_3 + iM_4$ — complex moment coefficient due to pitching oscillation, positive M_3 indicates moment acts leading edge down for positive α (moment opposes α) and positive M_4 indicates moment acts leading edge down for positive $\dot{\alpha}$ (moment opposes or damps $\dot{\alpha}$)

$\bar{L}_i$, $\bar{M}_i$ — components of total lift and moment coefficients for a pitch and moment axis at μ_0, appearing in equations (3) and (4), obtained by spanwise integration of L_i and M_i; $i = 1, 2, 3$, and 4

$\bar{L}_i'$, $\bar{M}_i'$ — parts of $\bar{L}_i$ and $\bar{M}_i$, defined by equations (6) and (7); $i = 1, 2, 3$, and 4

M free-stream Mach number, V/Speed of sound

M_α section moment per unit span on wing strip parallel to main stream, taken about axis of rotation μ_0, positive leading edge up

$\overline{M}_\alpha$ total moment on wing about axis of rotation μ_0, positive leading edge up, obtained by spanwise integration of M_α

P section force per unit span on wing strip parallel to main stream, positive downward

$\overline{P}$ total force on wing, positive downward, obtained by spanwise integration of P

r_α radius of gyration of rigid wing about axis at μ_0, nondimensional in terms of semichord b

t time

V velocity of main stream

α angular displacement about axis of rotation, positive leading edge up, $\alpha_0 e^{i\omega t}$

$\dot{\alpha} = \partial\alpha/\partial t$

α_0 amplitude of angular displacement about axis of rotation

$\alpha_i, \beta_i, \gamma_i, \delta_i$ functions of M and leading-edge sweep angle, defined following equations (7)

$\beta = \sqrt{M^2 - 1}$

ϵ half apex angle $(90^\circ - \Lambda)$

Λ, Λ_{TE} sweep angles of leading edge and trailing edge, respectively, positive for sweepback

μ, ν rectangular coordinates moving in negative μ-direction with average velocity of wing, nondimensional in terms of chord $2b$

μ_0 value of μ at axis of rotation and coincident moment axis of wing as shown in figure 1

μ_w mass ratio of wing, $\frac{\text{Wing mass}}{8\rho b^3 C}$

ω circular frequency of oscillation

$\bar{\omega}$ frequency parameter, $2kM^2/\beta^2$, nondimensional and equal to 2b times $\bar{\omega}$ in references 3 and 4

ρ air density in main stream

$\sigma = \beta^2 C^2 - 1$

σ_j constants depending on βC and M, defined following equation (5h); $j = 1, 2, \ldots 20$

EXPRESSIONS FOR TOTAL FORCE AND MOMENT

Expressions for the section lift and pitching moment for the thin arrowhead wing in vertical translation and pitch are given in reference 3 for the subsonic-leading-edge (narrow-wing) case and in reference 4 for the supersonic-leading-edge (wide-wing) case. Total forces and moments which can be useful in several applications, for example, flutter analyses of arrowhead wings or tails involving rigid-body components of motion, are obtained in the present paper by spanwise integration of the section lift and moment expressions. The plan form treated is that of the arrowhead wing shown in figure 1 with trailing edges swept forward or back and meeting the leading edge at a pointed tip; however, the component of flow velocity normal to the trailing edge must be supersonic or at least sonic.

The notations of references 3 and 4 have been followed herein insofar as possible; compromises have been made when differences exist between the two references. The section lift and the section moment about the axis $\mu = \mu_0$ are expressed by

$$P = -4\rho b V^2 k^2 e^{i\omega t}\left[\frac{h_0}{b}(L_1 + iL_2) + \alpha_0(L_3 + iL_4)\right] \tag{1}$$

$$M_\alpha = -4\rho b^2 V^2 k^2 e^{i\omega t}\left[\frac{h_0}{b}(M_1 + iM_2) + \alpha_0(M_3 + iM_4)\right] \tag{2}$$

(The axis about which the pitching oscillation takes place is also at $\mu = \mu_0$.)

The total lift and moment may be determined conveniently as twice the integral between the plane of symmetry and a wing tip and are

$$\bar{P} = 2\int_0^{Tip} P2b\, d\nu = -8\rho b^2 V^2 k^2 e^{i\omega t}\left[\frac{h_0}{b}\left(\bar{L}_1 + i\bar{L}_2\right) + \alpha_0\left(\bar{L}_3 + \bar{L}_4\right)\right] \tag{3}$$

$$\bar{M}_\alpha = 2\int_0^{Tip} M_\alpha 2b\, d\nu = -8\rho b^3 V^2 k^2 e^{i\omega t}\left[\frac{h_0}{b}\left(\bar{M}_1 + i\bar{M}_2\right) + \alpha_0\left(\bar{M}_3 + i\bar{M}_4\right)\right] \tag{4}$$

Subsonic-Leading-Edge Wing

Expressions for the section forces and moments are given in reference 3 for the subsonic-leading-edge arrowhead wing. The total forces and moments are the spanwise integrals of these section quantities. The spanwise coordinate y of reference 3 is replaced by ν, and the coordinate of the trailing edge x_1 is denoted herein by $1 + D\nu$, where D is the tangent of the trailing-edge sweep angle Λ_{TE}. The three basic integrals required, $I_{1,m}$, $I_{2,n}{}^m$, and $I_{3,n}$, are given in the appendix. With these integrals the coefficients of total force and moment (divided by C, the cotangent of the leading-edge sweep angle) can be written as

$$\frac{\bar{L}_1}{C} = \int_{Span} \frac{L_1}{C}\, d\nu$$

$$= 2\int_0^{\frac{C}{1-CD}} \frac{L_1}{C}\, d\nu$$

$$= \frac{2M^2\sigma_1 - \beta^2 A_0}{\beta^2} I_{2,1}{}^0 + \frac{A_0}{C^2} I_{3,2} + k^2 \frac{M^4}{\beta^4}\left[\frac{2}{\beta^2}\left(\beta^2\sigma_3 - 4M^2\sigma_5\right)I_{2,3}{}^0 + \left(4\beta^2\sigma_4 - \frac{\sigma_3}{C^2} - 8M^2\sigma_6\right)I_{2,1}{}^2 - \frac{1}{C^4}\left(\sigma_3 + 4\beta^2C^2\sigma_4\right)I_{3,4}\right] +$$

$$k^4 \frac{M^8}{\beta^8}\left[\frac{16}{3}\left(6\frac{M^2}{\beta^2}\sigma_{12} - \sigma_9\right)I_{2,5}{}^0 + \frac{4}{3}\left(24M^2\sigma_{13} + \frac{1}{C^2}\sigma_9 - 6\beta^2\sigma_{10}\right)I_{2,3}{}^2 + 32\beta^2\left(M^2\sigma_{14} - \beta^2\sigma_{11}\right)I_{2,1}{}^4 + \frac{2}{C^4}\left(\sigma_9 + 2\beta^2C^2\sigma_{10} + 8\beta^4C^4\sigma_{11}\right)\left(I_{2,1}{}^4 + \frac{1}{C^2}I_{3,6}\right)\right] \tag{5a}$$

$$\frac{\bar{L}_2}{c} = \frac{1}{k} A_0 I_{2,0}{}^0 + k \frac{M^2}{\beta^2}\left[\frac{4}{3\beta^2}\left(\beta^2\sigma_1 - 3M^2\sigma_3\right)I_{2,2}{}^0 - \frac{4}{3c^2}\left(3M^2c^2\sigma_4 + \sigma_1\right)I_{2,0}{}^2\right] +$$

$$k^3 \frac{M^6}{\beta^6}\left[\frac{16}{5\beta^2}\left(5M^2\sigma_9 - \beta^2\sigma_5\right)I_{2,4}{}^0 + \frac{16}{15c^2}\left(15M^2c^2\sigma_{10} + \sigma_5 - 5\beta^2c^2\sigma_6\right)I_{2,2}{}^2 +\right.$$

$$\left.\frac{16}{15c^4}\left(15M^2\beta^2c^4\sigma_{11} + 2\sigma_5 + 5\beta^2c^2\sigma_6\right)I_{2,0}{}^4\right] \tag{5b}$$

$$\frac{\bar{L}_3}{c} = \frac{1}{k}\frac{\bar{L}_2}{c} + \frac{4}{3\beta^2}\left(3M^2\sigma_2 - \beta^2A_1\right)I_{2,2}{}^0 + \frac{4}{3c^2}\left(A_1 - 3M^2c^2A_3\right)I_{2,0}{}^2 +$$

$$k^2 \frac{M^4}{\beta^4}\left[\frac{16}{5\beta^2}\left(\beta^2\sigma_7 - 5M^2\sigma_{15}\right)I_{2,4}{}^0 - \frac{16}{15c^2}\left(15M^2c^2\sigma_{16} + \sigma_7 + 5\beta^2c^2\sigma_8\right)I_{2,2}{}^2 +\right.$$

$$\left.\frac{16}{15c^4}\left(5\beta^2c^2\sigma_8 - 2\sigma_7 - 15M^2\beta^2c^4\sigma_{17}\right)I_{2,0}{}^4\right] - 2\mu_0\frac{\bar{L}_1}{c} \tag{5c}$$

$$\frac{\bar{L}_4}{c} = -\frac{1}{k}\frac{\bar{L}_1}{c} + \frac{1}{k}2A_1I_{2,1}{}^0 + k\frac{M^2}{\beta^2}\left[\frac{2}{\beta^2}\left(\beta^2\sigma_2 - 4M^2\sigma_7\right)I_{2,3}{}^0 +\right.$$

$$\left.\frac{1}{c^2}\left(8M^2c^2\sigma_8 - \sigma_2 - 4\beta^2c^2A_3\right)I_{2,1}{}^2 + \frac{1}{c^4}\left(4\beta^2c^2A_3 - \sigma_2\right)I_{3,4}\right] +$$

$$k^3\frac{M^6}{\beta^6}\left[\frac{16}{3\beta^2}\left(6M^2\sigma_{18} - \beta^2\sigma_{15}\right)I_{2,5}{}^0 + \frac{4}{3c^2}\left(24M^2c^2\sigma_{19} - 6\beta^2c^2\sigma_{16} +\right.\right.$$

$$\left.\sigma_{15}\right)I_{2,3}{}^2 + 32\beta^2\left(M^2\sigma_{20} - \beta^2\sigma_{17}\right)I_{2,1}{}^4 + \frac{2}{c^4}\left(\sigma_{15} + 2\beta^2c^2\sigma_{16} +\right.$$

$$\left.\left.8\beta^4c^4\sigma_{17}\right)\left(I_{2,1}{}^4 + \frac{1}{c^2}I_{3,6}\right)\right] - 2\mu_0\frac{\bar{L}_2}{c} \tag{5d}$$

$$\frac{\bar{M}_1}{c} = \frac{4}{3\beta^2}\left(2M^2\sigma_1 - \beta^2 A_0\right)I_{2,2}{}^0 + \frac{4}{3\beta^2c^2}\left(M^2\sigma_1 + \beta^2 A_0\right)I_{2,0}{}^2 + k^2\frac{M^4}{\beta^6}\left[\frac{16}{5}\left(-4M^2\sigma_5 + \beta^2\sigma_3\right)I_{2,4}{}^0 - \frac{16}{15c^2}\left(\beta^2\sigma_3 - 5\beta^4c^2\sigma_4 + M^2\sigma_5 + 10M^2\beta^2c^2\sigma_6\right)I_{2,2}{}^2 + \frac{-16}{15c^4}\left(2\beta^2\sigma_3 + 5\beta^4c^2\sigma_4 + 2M^2\sigma_5 + 5M^2\beta^2c^2\sigma_6\right)I_{2,0}{}^4\right] + k^4\frac{M^8}{\beta^{10}}\left[\frac{64}{7}\left(-\beta^2\sigma_9 + 6M^2\sigma_{12}\right)I_{2,6}{}^0 + \frac{64}{35c^2}\left(\beta^2\sigma_9 - 7\beta^4c^2\sigma_{10} + M^2\sigma_{12} + 28M^2\beta^2c^2\sigma_{13}\right)I_{2,4}{}^2 + \frac{64}{105c^4}\left(4\beta^2\sigma_9 + 7\beta^4c^2\sigma_{10} - 35\beta^6c^4\sigma_{11} + 4M^2\sigma_{12} + 7M^2\beta^2c^2\sigma_{13} + 70M^2\beta^4c^4\sigma_{14}\right)\left(\frac{2}{c^2}I_{2,0}{}^6 + I_{2,2}{}^4\right) + 64\frac{\beta^4}{c^2}\left(\beta^2\sigma_{11} - M^2\sigma_{14}\right)I_{2,0}{}^6\right] - 2\mu_0\frac{\bar{I}_1}{c} \tag{5e}$$

$$\frac{\bar{M}_2}{c} = \frac{1}{k}\left[A_0\left(I_{2,1}{}^0 + \frac{1}{c^2}I_{3,2}\right)\right] + k\frac{M^2}{\beta^4}\left[2\left(\beta^2\sigma_1 - 3M^2\sigma_3\right)I_{2,3}{}^0 - \frac{1}{c^2}\left(\beta^2\sigma_1 + M^2\sigma_3 + 4M^2\beta^2c^2\sigma_4\right)\left(I_{2,1}{}^2 + \frac{1}{c^2}I_{3,4}\right)\right] + k^3\frac{M^6}{\beta^8}\left[\frac{16}{3}\left(5M^2\sigma_9 - \beta^2\sigma_5\right)I_{2,5}{}^0 + \frac{4}{3c^2}\left(\beta^2\sigma_5 - 6\beta^4c^2\sigma_6 + M^2\sigma_9 + 18M^2\beta^2c^2\sigma_{10}\right)I_{2,3}{}^2 + \frac{2}{c^4}\left(\beta^2\sigma_5 + 2\beta^4c^2\sigma_6 + M^2\sigma_9 + 2M^2\beta^2c^2\sigma_{10} + 8M^2\beta^4c^4\sigma_{11}\right)\left(I_{2,1}{}^4 + \frac{1}{c^2}I_{3,6}\right)\right] - 2\mu_0\frac{\bar{I}_2}{c} \tag{5f}$$

$$\frac{\bar{M}_3}{c} = \frac{1}{k}\frac{\bar{M}_2}{c} + \frac{2}{\beta^2}\left(3M^2\sigma_2 - \beta^2 A_1\right)I_{2,3}{}^0 + \frac{1}{\beta^2 c^2}\left(\beta^2 A_1 + M^2\sigma_2 - 4M^2\beta^2 c^2 A_3\right)\left(I_{2,1}{}^2 + \frac{1}{c^2} I_{3,4}\right) + k^2 \frac{M^4}{\beta^6}\left[\frac{16}{3}\left(\beta^2\sigma_7 - 5M^2\sigma_{15}\right)I_{2,5}{}^0 - \frac{4}{3c^2}\left(\beta^2\sigma_7 + 6\beta^4 c^2\sigma_8 + M^2\sigma_{15} + 18M^2\beta^2 c^2\sigma_{16}\right)I_{2,3}{}^2 - \frac{2}{c^4}\left(\beta^2\sigma_7 - 2\beta^4 c^2\sigma_8 + M^2\sigma_{15} + 2M^2\beta^2 c^2\sigma_{16} + 8M^2\beta^4 c^4\sigma_{17}\right)\left(I_{2,1}{}^4 + \frac{1}{c^2} I_{3,6}\right)\right] - 2\mu_0\left(\frac{\bar{M}_1}{c} + \frac{\bar{I}_3}{c} + 2\mu_0\frac{\bar{I}_1}{c}\right) \tag{5g}$$

$$\frac{\bar{M}_4}{c} = -\frac{1}{k}\frac{\bar{M}_1}{c} + \frac{1}{k}\left[\frac{4A_1}{3}\left(2I_{2,2}{}^0 + \frac{1}{c^2} I_{2,0}{}^2\right)\right] + k\frac{M^2}{\beta^4}\left[\frac{16}{5}\left(\beta^2\sigma_2 - 4M^2\sigma_7\right)I_{2,4}{}^0 + \frac{16}{15c^2}\left(-\beta^2\sigma_2 - 5\beta^4 c^2 A_3 - M^2\sigma_7 + 10M^2\beta^2 c^2\sigma_8\right)\left(I_{2,2}{}^2 + \frac{2}{c^2} I_{2,0}{}^4\right) + \frac{16}{c^2}\left(\beta^2 A_3 - M^2\sigma_8\right)I_{2,0}{}^4\right] + k^3\frac{M^6}{\beta^8}\left[\frac{64}{7}\left(6M^2\sigma_{18} - \beta^2\sigma_{15}\right)I_{2,6}{}^0 + \frac{64}{35c^2}\left(\beta^2\sigma_{15} - 7\beta^4 c^2\sigma_{16} + M^2\sigma_{18} + 28M^2\beta^2 c^2\sigma_{19}\right)I_{2,4}{}^2 + \frac{64}{105c^4}\left(4\beta^2\sigma_{15} + 7\beta^4 c^2\sigma_{16} - 35\beta^6 c^4\sigma_{17} + 4M^2\sigma_{18} + 7M^2\beta^2 c^2\sigma_{19} + 70M^2\beta^4 c^4\sigma_{20}\right)\left(I_{2,2}{}^4 + \frac{2}{c^2} I_{2,0}{}^6\right) + \frac{64\beta^2}{c^2}\left(M^4\sigma_{14} + \beta^4\sigma_{17} - M^2\beta^2\sigma_{20}\right)I_{2,0}{}^6\right] - 2\mu_0\left(\frac{\bar{M}_2}{c} + \frac{\bar{I}_4}{c} + 2\mu_0\frac{\bar{I}_2}{c}\right) \tag{5h}$$

where

$$\sigma_j = P_j + \frac{Q_j}{M^2} + \frac{R_j}{M^4}$$

The quantities A_1, P_j, Q_j, and R_j are defined and tabulated in reference 3.

Supersonic-Leading-Edge Wing

Expressions for the section forces and moments are given in reference 4 for the supersonic-leading-edge arrowhead wing. The spanwise integrals of these section quantities are the total forces and moments. The section coefficients are expressed in terms of the spanwise variables E_{mn}, F_{mn}^{e}, G_{mn}, and H_{mn}^{e}. Their spanwise integrals $\bar{E}_{mn}$, $\bar{F}_{mn}^{e}$, $\bar{G}_{mn}$, and $\bar{H}_{mn}^{e}$ are given in the appendix. The coefficients of total force and moment can be written as

$$\left.\begin{aligned}
\bar{L}_1 + i\bar{L}_2 &= \bar{L}_1' + i\bar{L}_2' \\
\bar{L}_3 + i\bar{L}_4 &= \bar{L}_3' + i\bar{L}_4' - \left(\frac{i}{k} + 2\mu_0\right)\left(\bar{L}_1 + i\bar{L}_2\right) \\
\bar{M}_1 + i\bar{M}_2 &= \bar{M}_1' + i\bar{M}_2' - 2\mu_0\left(\bar{L}_1 + i\bar{L}_2\right) \\
\bar{M}_3 + i\bar{M}_4 &= \bar{M}_3' + i\bar{M}_4' - 2\mu_0\left(\bar{L}_3' + i\bar{L}_4'\right) - \left(\frac{i}{k} + 2\mu_0\right)\left(\bar{M}_1 + i\bar{M}_2\right)
\end{aligned}\right\} \tag{6}$$

where

$$-2\pi\bar{L}_1 = \alpha_1\bar{E}_{01} + \beta_1\bar{H}_{01}^{\,0} + \beta_2\bar{F}_{02}^{\,0} + k^2\left(\alpha_2\bar{G}_{02} + \alpha_3\bar{G}_{20} + \alpha_4\bar{E}_{03} + \alpha_5\bar{E}_{21} + \beta_3\bar{H}_{03}^{\,0} + \beta_4\bar{F}_{04}^{\,0}\right) \tag{7a}$$

$$-2\pi\bar{L}_2 = -\beta_1\bar{F}_{01}^{\,0}\frac{1}{k} + k\left(\alpha_1\bar{G}_{01} - \alpha_2\bar{E}_{02} - \alpha_3\bar{E}_{20} + \beta_2\bar{H}_{02}^{\,0} - \beta_3\bar{F}_{03}^{\,0}\right) \tag{7b}$$

$$-2\pi\bar{L}_3' = \gamma_1\bar{G}_{01} + \gamma_2\bar{E}_{02} + \gamma_3\bar{E}_{20} + \delta_1\bar{H}_{11}{}^0 + \delta_2\bar{H}_{01}{}^1 + \delta_3\bar{H}_{02}{}^0 + \delta_4\bar{F}_{12}{}^0 + \delta_5\bar{F}_{03}{}^0 \tag{7c}$$

$$-2\pi\bar{L}_4' = -\frac{1}{k}\left(\gamma_1\bar{E}_{01} + \delta_1\bar{F}_{11}{}^0 + \delta_2\bar{F}_{01}{}^1 + \delta_3\bar{F}_{02}{}^0\right) + k\left(\gamma_2\bar{G}_{02} + \gamma_3\bar{G}_{20} - \gamma_4\bar{E}_{03} - \gamma_5\bar{E}_{21} + \delta_4\bar{H}_{12}{}^0 + \delta_5\bar{H}_{03}{}^0 - \delta_6\bar{F}_{13}{}^0 - \delta_7\bar{F}_{03}{}^1 - \delta_8\bar{F}_{04}{}^0\right) \tag{7d}$$

$$-2\pi\bar{M}_1' = \left[\alpha_1\left(\bar{E}_{02} - \bar{G}_{01}\right) + \beta_1\bar{H}_{11}{}^0 + \beta_2\left(\bar{F}_{12}{}^0 - \bar{H}_{02}{}^0\right)\right] + k^2\left[\alpha_2\bar{G}_{03} + \alpha_3\bar{G}_{21} + \alpha_4\left(\bar{E}_{04} - \bar{G}_{03}\right) + \alpha_5\left(\bar{E}_{22} - \bar{G}_{21}\right) + \beta_3\bar{H}_{13}{}^0 + \beta_4\left(\bar{F}_{14}{}^0 - \bar{H}_{04}{}^0\right)\right] \tag{7e}$$

$$-2\pi\bar{M}_2' = \beta_1\left(\bar{H}_{01}{}^0 - \bar{F}_{11}{}^0\right)\frac{1}{k} + k\left[\alpha_1\bar{G}_{02} + \alpha_2\left(\bar{G}_{02} - \bar{E}_{03}\right) + \alpha_3\left(\bar{G}_{20} - \bar{E}_{21}\right) + \beta_2\bar{H}_{12}{}^0 + \beta_3\left(\bar{H}_{03}{}^0 - \bar{F}_{13}{}^0\right)\right] \tag{7f}$$

$$-2\pi\bar{M}_3' = \gamma_1\bar{G}_{02} + \gamma_2\left(\bar{E}_{03} - \bar{G}_{02}\right) + \gamma_3\left(\bar{E}_{21} - \bar{G}_{20}\right) + \delta_1\bar{H}_{21}{}^0 + \delta_2\bar{H}_{11}{}^1 + \delta_3\bar{H}_{12}{}^0 + \delta_4\left(\bar{F}_{22}{}^0 - \bar{H}_{12}{}^0\right) + \delta_5\left(\bar{F}_{13}{}^0 - \bar{H}_{03}{}^0\right) \tag{7g}$$

$$-2\pi\bar{M}_4' = \frac{1}{k}\left[\gamma_1\left(\bar{G}_{01} - \bar{E}_{02}\right) + \delta_1\left(\bar{H}_{11}{}^{0} - \bar{F}_{21}{}^{0}\right) + \delta_2\left(\bar{H}_{01}{}^{1} - \bar{F}_{11}{}^{1}\right) + \delta_3\left(\bar{H}_{02}{}^{0} - \bar{F}_{12}{}^{0}\right)\right] + k\left[\gamma_2\bar{G}_{03} + \gamma_3\bar{G}_{21} + \gamma_4\left(\bar{G}_{03} - \bar{E}_{04}\right) + \gamma_5\left(\bar{G}_{21} - \bar{E}_{22}\right) + \delta_4\bar{H}_{22}{}^{0} + \delta_5\bar{H}_{13}{}^{0} + \delta_6\left(\bar{H}_{13}{}^{0} - \bar{F}_{23}{}^{0}\right) + \delta_7\left(\bar{H}_{03}{}^{1} - \bar{F}_{13}{}^{1}\right) + \delta_8\left(\bar{H}_{04}{}^{0} - \bar{F}_{14}{}^{0}\right)\right] \tag{7h}$$

where, as in reference 4, but with C replacing λ,

$$\alpha_1 = \frac{M^2C}{\beta^2\sigma}$$

$$\alpha_2 = \frac{M^2C}{6\beta^4\sigma^2}\left[M^2(4\sigma + 3) + \sigma\right]$$

$$\alpha_3 = \frac{M^2C}{6\beta^2\sigma^2}\left(3M^2 + \sigma\right)$$

$$\alpha_4 = \frac{-M^4C}{72\beta^6\sigma^3}\left[M^2\left(18\sigma^2 + 31\sigma + 15\right) + 3\sigma(5\sigma + 3)\right]$$

$$\alpha_5 = \frac{-M^4C}{72\beta^4\sigma^3}\left[M^2(38\sigma + 45) + 3\sigma(4\sigma + 9)\right]$$

$$\beta_1 = \frac{1}{\sqrt{\sigma}} \qquad \beta_3 = \frac{-M^2}{12\beta^2\sigma^{5/2}}\left[M^2(2\sigma + 3) + \sigma\right]$$

$$\beta_2 = -\frac{M^2C}{2\sigma^{3/2}} \qquad \beta_4 = \frac{M^4C}{48\beta^2\sigma^{7/2}}\left[M^2(2\sigma + 5) + 3\sigma\right]$$

$$\gamma_1 = \frac{C}{\sigma} \qquad \gamma_3 = -\frac{M^2C}{\sigma^2}$$

$$\gamma_2 = \frac{-M^2C}{3\beta^2\sigma^2}(\sigma + 3) \qquad \gamma_4 = \frac{-M^2C}{24\beta^4\sigma^3}\left[M^2\left(2\sigma^2 + 19\sigma + 15\right) + \sigma(\sigma + 3)\right]$$

$$\gamma_5 = \frac{-M^2C}{24\beta^2\sigma^3}\left[M^2(26\sigma + 45) + 9\sigma\right]$$

$$\delta_1 = -\frac{1}{\sigma^{3/2}} \qquad \delta_5 = \frac{M^2}{6\sigma^{5/2}}(2\sigma + 3)$$

$$\delta_2 = \delta_1 \qquad \delta_6 = \frac{M^2}{48\beta^2\sigma^{7/2}}\left[4M^2(4\sigma + 5) + \sigma(3 - \sigma)\right]$$

$$\delta_3 = \frac{\beta^2C}{2\sigma^{3/2}} \qquad \delta_7 = \frac{M^2}{48\beta^2\sigma^{7/2}}\left[4M^2(2\sigma + 5) + 3\sigma\right]$$

$$\sigma_4 = \frac{-M^2C}{2\sigma^{3/2}} \qquad \delta_8 = \frac{-M^4C}{48\sigma^{7/2}}(2\sigma + 5)$$

It is to be noted for the supersonic-leading-edge wing that, as the sonic-leading-edge limit is approached, all the coefficients α_i, β_i, γ_i, and δ_i approach infinite values because σ approaches zero. For the condition, therefore, of a slightly supersonic leading edge, a large number of significant figures would have to be used because of the loss of significant figures at the final step (eqs. (7)). For the limiting condition the force and moment coefficients of equations (7) are finite differences of infinite quantities and their numerical determination by the present expressions cannot be made. The sonic-leading-edge wing remains entirely tractable, however, as a limiting condition of the subsonic-leading-edge wing.

In this section on the supersonic-leading-edge wing, a point concerning only the delta plan form, made in references 1 and 4, bears repeating; namely, the total coefficients divided by C $\left(\bar{L}_1/C,\ \bar{L}_2/C,\right.$ etc.$\left.\right)$ are dependent only on Mach number and not on C. This means that,

for Mach numbers at which it may be inconvenient to obtain the exact results of reference 1, flutter coefficients (divided by C) can be obtained to the fifth power of the frequency as follows: At the Mach number of interest, calculate the coefficients, $\bar{L}_1/C$, and so forth, for a delta wing with sonic leading edges from the expressions for the subsonic-leading-edge wing. For constant M these quantities remain unchanged for all the wider supersonic-leading-edge wings. This same observation does not apply to the total coefficients if the trailing edge is swept, nor does it apply to the section force and moment coefficients for any arrowhead plan form.

The sections to follow give some observations drawn from determination and use of the flutter coefficients obtained from the expressions of this and the preceding sections.

RESULTS AND DISCUSSION

Effects of Mach Number, Plan Form, and Pitch-Axis Location

In order that some effects of parameter variations can be observed, sets of force and moment coefficients are presented in tables I to III. Table I is arranged in the order of increasing Mach number for a specific wing plan form. Tables II(a) and II(b) are arranged in the order of increasing leading-edge sweep angle, with Mach number and trailing-edge sweep angle held constant (or essentially constant). Table III is arranged in the order of decreasing trailing-edge sweep angle (sweepback is positive) with Mach number and leading-edge sweep angle held constant. The purpose of the arrangement of the tables is to show that, for any given reduced frequency k, the higher order frequency terms become progressively less important compared with the lowest order frequency term for any of the following parametric changes: increasing Mach number, increasing leading-edge sweep angle (except for the supersonic-leading-edge delta wing, as noted previously), or decreasing trailing-edge sweep angle.

In order to show some effects of Mach number, plan form, and pitch-axis location on single-degree pitching instability, figure 2 is presented. Boundaries separating stable and unstable regions of Mach number and pitch-axis location are given for arrowhead wings with 45° sweptback leading edges and with five different trailing-edge sweeps, including 0° sweep obtained from figure 7 of reference 3. The regions of possible pitching instability lie below the respective curves and sweepback of the trailing edge is seen to be unfavorable or destabilizing, whereas sweepforward has the opposite effect. The various curves have not been extended below the Mach number at which the trailing edge is sonic. The curves apply to slow oscillations for which terms in $\bar{M}_4$ other than the

1/k term are negligible. If the frequency were to increase, the unstable region would shrink downward.

In order to provide some insight into the reason why sweepback of the trailing edge can have a destabilizing effect, figure 3 shows the regions on arrowhead wings which experience a destabilizing pressure component for low-frequency pitching oscillations; that is, at the instant in a cycle of a pitching oscillation when the pitching velocity is a positive maximum (and displacement is zero), the hatched regions of figure 3 have a pressure difference acting in the direction of the local translational velocity of the surface. These regions may also be said to have a pressure which leads the pitching displacement. For convenience, only one-half of the wing is shown, because the pressure distribution is symmetric about the root chord.

Wings with two different leading-edge sweep angles are shown, 45° and 60°, for a Mach number of 10/9 and with various pitch-axis locations as indicated in figure 3. It is to be noted from the figure that, for an axis location behind the 49 percent root chord on the 45° wing and behind the 73 percent root chord on the 60° wing, essentially all wing area added between the pitch axis and trailing edge by sweeping the trailing edge back is destabilizing. For more forward axis locations, some stabilizing and some destabilizing area is added by trailing-edge sweepback, with the net contribution being in the destabilizing direction unless the pitch axis is well forward, as would be the case, for example, for a noncanard horizontal tail.

As has been pointed out, figure 2 shows regions of possible pitching instability for certain plan forms. Before a pitching instability of an arrowhead-wing aircraft (without an oscillating control surface) can actually occur, however, other conditions on mass, mass moment, and elastic restraint must be satisfied. In order to illustrate some of these conditions, the simple case of a rigid arrowhead wing flying freely has been analyzed and the results are presented in figure 4 for a Mach number of approximately 1.25 with the center of gravity (and pitch and moment axis) at the root midchord $\left(\mu_0 = 0.5\right)$. The conditions on the wing are that it has two longitudinal degrees of freedom, pitching and vertical translation (but no freedom to vary its speed in the fore-and-aft direction), and is not elastically restrained; also, no effects of gravity, thrust, or aerodynamic forces due to a fuselage or to the thickness of the wing are considered. The dynamical equations of equilibrium for harmonic oscillations about the center of gravity can be expressed simply in matrix form as

$$\begin{bmatrix} \mu_w - \left(\frac{\bar{L}_1}{c} + i\frac{\bar{L}_2}{c}\right) & -\left(\frac{\bar{L}_3}{c} + i\frac{\bar{L}_4}{c}\right) \\ -\left(\frac{\bar{M}_1}{c} + i\frac{\bar{M}_2}{c}\right) & r_\alpha^2\mu_w - \left(\frac{\bar{M}_3}{c} + i\frac{\bar{M}_4}{c}\right) \end{bmatrix} \begin{bmatrix} \frac{h_0}{b} \\ \alpha_0 \end{bmatrix} = \begin{bmatrix} 0 \\ 0 \end{bmatrix} \tag{8}$$

The quantities h_0 and α_0 are the complex amplitudes of harmonic motion of vertical translation and of pitch, respectively; μ_w and r_α are described in the next paragraph.

The nontrivial solution of equation (8) can be obtained by setting the determinant of the four-element square matrix equal to zero. The abscissa μ_w of figure 4 is the ratio of the mass of the wing to the mass of air $\rho(2b)^3C$. As an airplane gains altitude, its mass ratio moves to the right in figure 4. The ordinate r_α is the radius of gyration in pitch of the subject arrowhead wing, nondimensionalized in terms of the root semichord; that is, r_α is unity if the radius of gyration is equal to the semichord b. The three plan forms represented in figure 4 have subsonic or sonic leading edges, and the solid curves are the result of using coefficients which include the fifth power of the frequency.

The unstable regions are inside and to the right of the respective curves. The lower right-hand curve applies to a delta wing with a leading-edge sweep angle of 45°. When the trailing edge is swept back 20°, with the leading-edge sweep angle held at 45°, the unstable region expands upward to the highest curve shown. (Fig. 2 also has curves for these two plan forms.) If, instead of the trailing-edge sweep angle being increased, the leading-edge sweep angle is decreased to the point where that edge is sonic ($\Lambda = 36.8°$), the region of instability extends outward to the curve farthest to the left. (The short-dash curve labeled "Exact (ref. 1)" and the long-dash curve resulting from first-order frequency coefficients for the same plan form are discussed in the next section.) If the Mach number changes from that of figure 4, the unstable regions expand to the left as M decreases and shrink to the right and eventually vanish as M increases. Location of the pitch axis also affects the extent of the unstable region. No unstable region exists in a plot of the type of figure 4 unless the wing has a plan form, a Mach number, and a pitch-axis location which fall in a region of possible instability in a plot of the type of figure 2. A rigid arrowhead wing flying at supersonic speed with the two specified degrees of freedom therefore can experience an oscillatory instability only if it falls in unstable regions of plots of the types of both figure 2 and figure 4.

Comparisons With Other Work

Comparisons of results from the expressions of the present paper can be made with the exact results of reference 1 only for the case of the supersonic-leading-edge (wide) delta plan form. (In ref. 1 the tabulated values of the Schwarz function f_4 are incorrect and, as a result, the coefficients R_{M_α}, $-(1/k)I_{M_\alpha}$, and $-I_{l_\phi}$ are inaccurate. In the present paper wherever numerical results from the theoretical analysis of ref. 1 are plotted, corrected values are used.)

Comparisons of the present results can also be made with the first-order frequency coefficients generally used in dynamic-stability work. It can be shown that the stability coefficients are identical with coefficients resulting from a frequency power-series expansion of the velocity potential which includes only the zero and first power of the frequency (and the second power for vertical translation since the unit of translation here is h and not $\dot{h}$); these zero- and first-power terms therefore result in the steady-state and steady-rate-of-change coefficients, respectively. In the force and moment coefficients of equations (5) and (7) the zero-order-of-the-frequency or static stability coefficients are the terms involving $1/k^2$ in $\bar{L}_3$ and $\bar{M}_3$ (a k^2-multiplier is taken outside in eqs. (3) and (4)) and those involving $1/k$ in $\bar{L}_2$ and $\bar{M}_2$. (The latter terms would also involve $1/k^2$ if the unit of translation were the translational velocity $\dot{h}$ as in airplane stability work rather than the translational displacement h used in flutter work.) Addition of the terms involving $1/k$ in $\bar{L}_4$ and $\bar{M}_4$ and those involving k to the zero power in $\bar{L}_1$ and $\bar{M}_1$ gives the first-order-of-the-frequency or quasi-steady dynamic stability coefficients. Equations (5) and (7) include all terms to the fifth power and the third power, respectively, of the frequency.

Table IV lists the notation for the coefficients of the present paper along with the corresponding notation of reference 1 and of reference 5 for an arbitrary fore-and-aft location of pitch and moment axis. The quantities on any one line approach exact numerical equality as the frequency of oscillation approaches zero. It should be pointed out that the reference length in the present flutter work is the root chord $2b$, whereas the reference length in stability work is the mean aerodynamic chord $\bar{c}$ which, for arrowhead wings, is $(2/3)(2b)$.

The accuracy of the approximate coefficients extending to the third and to the fifth powers of the frequency can be compared with the exact results of reference 1. The frequency range in which the approximate coefficients are sufficiently accurate is the smallest for low supersonic

Mach numbers. For this reason one Mach number chosen as a basis of comparison is $M = 10/9$; comparison is also made at $M = 10/7$. The results are presented in figure 5 as functions of the frequency parameter $\bar{\omega} = \frac{2kM^2}{M^2 - 1}$ for a pitch-axis location at the root midchord $(\mu_0 = 0.5)$. The accuracy can be assessed from the figure and it can be readily seen that, for each force and moment coefficient, the more terms carried in the power series, the more closely the approximate curve follows the exact curve. The lowest order frequency term, represented by a horizontal line in each part of figure 5, illustrates the corresponding coefficient of dynamic-stability work, useful for sufficiently low frequencies. If an inaccuracy of 10 percent from the exact values can be tolerated, the approximations adequately represent the exact theory in ranges of the frequency parameter $\bar{\omega}$ as follows: For expansion of the velocity potential to $\bar{\omega}^3$, the range of usefulness is about $0 \leqq \bar{\omega} \leqq 1.4$. For expansion to $\bar{\omega}^5$, the range is limited by $\bar{M}_3$ to about $0 \leqq \bar{\omega} \leqq 1.7$. For the dynamic stability coefficients (expansion to $\bar{\omega}$) the range is about $0 \leqq \bar{\omega} \leqq 0.7$, which, for this Mach number of 10/9, represents an oscillation as rapid as 95 root chords (142 mean aerodynamic chords) per cycle. The wave length in root chords is equal to π/k. (It should be understood that for certain combinations of plan form, Mach number, and pitch-axis location (for example, as shown in fig. 2) the first-order approximation to the damping in pitch $\bar{M}_4$ can be zero or near zero, in which case the higher order contributions even at low frequencies can be a large percent of the first-order contribution. The fact remains, however, that the higher order contributions are small in absolute amount for low frequencies and vanish at the limit of zero frequency.)

As the Mach number decreases toward unity, the useful range of reduced frequency k decreases toward zero since $k = \frac{\bar{\omega}(M^2 - 1)}{2M^2}$; furthermore, the usefulness of the linearized theory itself becomes questionable as M approaches unity. Conversely, as M increases, the useful range of k increases even if the useful range of $\bar{\omega}$ remains constant. The useful range of $\bar{\omega}$ may increase, however, as M increases, as is illustrated in figure 5 by comparison of the coefficient curves for $M = 10/7$ with those for $M = 10/9$, both cases being for the supersonic-leading-edge delta wing. It can be seen that for the higher Mach number the approximate curves are more closely grouped about the exact curve for most of the coefficients, notably $k\bar{L}_2/C$ and $k^2\bar{M}_3/C$.

A point to be noted from the curves of $k\bar{M}_4/C$ is that this quantity, representing the damping of pitching oscillations, increases with an

increase in frequency; this result indicates that higher reduced frequencies have a stabilizing effect on the pitching degree of freedom.

The immediately preceding paragraphs discussing figure 5 are concerned with the accuracy of the approximate coefficients specifically for the sonic- and supersonic-leading-edge delta plan forms at $M = 10/9$ and $M = 10/7$. In a broader vein it was pointed out in the preceding section with the aid of tables I, II, and III that, for the arrowhead wing in general, increasing the Mach number, increasing the leading-edge sweep angle (except for the supersonic-leading-edge delta wing), or decreasing the trailing-edge sweep angle has the effect of decreasing the relative importance of the higher order frequency terms in comparison with the lowest order frequency term in each flutter coefficient. A concurrent result is, of course, that any of these given parametric changes brings about an increased accuracy for the approximate coefficients of the present paper as well as for the results of references 3 to 8.

In figure 4 a short-dash curve is included for comparison; this curve results from use of the exact coefficients of reference 1 for the case of the sonic-leading-edge delta wing at $M = 1.25$. The wing plan form and Mach number for the short-dash curve and the associated solid curve are identical, and it may be seen that the approximate curve (fifth power of the frequency) is very close to the exact curve. As a matter of interest, the long-dash curve labeled "$\bar{\omega}$" shows the corresponding result of applying first-power-of-the-frequency coefficients. As this long-dash curve extends to the left, it shows to an increasing extent a result of misapplying the first-power frequency coefficients to too high values of oscillation frequency.

CONCLUDING REMARKS

Expressions based on linearized supersonic potential theory are given for the total forces and moments on thin rigid arrowhead wings oscillating harmonically in pitch and vertical translation. These expressions are based on an expansion of the velocity potential as a power series in terms of the frequency of oscillation and extend to the fifth power of the frequency for the subsonic-leading-edge wing and to the third power for the supersonic-leading-edge wing. Figures are presented from which the accuracy of these expressions can be assessed.

The importance of higher order frequency terms in the flutter coefficients in comparison with the lowest order frequency term decreases in general as the following parametric changes occur: increasing Mach number, increasing leading-edge sweep angle (except for the supersonic-leading-edge delta wing), and decreasing trailing-edge sweep angle.

Such parametric changes have the concurrent result that the approximate results of the present paper, as well as those of NACA Technical Note 2494 and NACA Report 1099 (which give section coefficients for supersonic- and subsonic-leading-edge arrowhead wings, respectively), become increasingly accurate for any given reduced frequency.

With regard to dynamic instability in pitch, for a given Mach number, pitch-axis location, and leading-edge sweep angle, an arrowhead wing is more stable (or less unstable) if the trailing edge is sweptforward and less stable if the trailing edge is sweptback. The wing also tends to be more stable at higher frequencies than at low frequencies. An instability in pitch, however, does not necessarily imply an instability if the wing is also free to translate vertically. Examples are shown of requirements on mass ratio and radius of gyration for the condition of no elastic restraint, that is, with the wing flying freely, with these two degrees of freedom.

Langley Aeronautical Laboratory,
National Advisory Committee for Aeronautics,
Langley Field, Va., February 3, 1955.

APPENDIX

SPANWISE INTEGRALS

Subsonic-Leading-Edge Wing

For use in equations (5a) to (5h), several spanwise integrals are required. The first is

$$I_{1,m} = 2\int_0^{\frac{C}{1-CD}} \nu^m \sqrt{1 + 2D\nu + \left(D^2 - \frac{1}{C^2}\right)\nu^2}\, d\nu \qquad (A1)$$

where $C = \cot \Lambda$ and $D = \tan \Lambda_{TE}$. By use of a recursion formula,

$$I_{1,m} = \frac{1}{m+2} \frac{C^2}{1 - C^2D^2}\left[(2m + 1)DI_{1,m-1} + (m - 1)I_{1,m-2}\right] \qquad (m \geq 2) \quad (A2)$$

with

$$I_{1,0} = \frac{C^2}{1 - C^2D^2}\left[\frac{1}{C\sqrt{1 - C^2D^2}}\left(\frac{\pi}{2} + \sin^{-1}CD\right) + D\right] \qquad (m = 0) \quad (A3)$$

$$I_{1,1} = \frac{1}{3} \frac{C^2}{1 - C^2D^2}\left(2 + 3DI_{1,0}\right) \qquad (m = 1) \quad (A4)$$

Another integral needed is

$$I_{2,n}{}^m = 2\int_0^{\frac{C}{1-CD}} \nu^m(1 + D\nu)^n \sqrt{1 + 2D\nu + \left(D^2 - \frac{1}{C^2}\right)\nu^2}\, d\nu \qquad (A5)$$

which can be determined from combinations of various values of $I_{1,m}$ when $(1 + D\nu)^n$ is expanded or, for the case of $m = 0$, can be found by use of the recursion formula

$$I_{2,n}{}^0 = 2\int_0^{\frac{C}{1-CD}} (1 + D\nu)^n \sqrt{1 + 2D\nu + \left(D^2 - \frac{1}{C^2}\right)\nu^2}\, d\nu$$

$$= \frac{C^2}{(n + 2)\left(1 - C^2D^2\right)} \left\{ \frac{1}{C^2}\left[(2n + 1)I_{2,n-1}{}^0 - (n - 1)I_{2,n-2}{}^0\right] + 2D \right\}$$

$$(n \geqq 1) \qquad \text{(A6)}$$

and, for $n = 0$, $I_{2,0}{}^0 = I_{1,0}$.

The third integral needed is

$$I_{3,n} = 2\int_0^{\frac{C}{1-CD}} \nu^n \cosh^{-1} \frac{C(1 + D\nu)}{\nu}\, d\nu \qquad \text{(A7)}$$

Through integration by parts,

$$I_{3,n} = \frac{2}{n + 1}\int_0^{\frac{C}{1-CD}} \frac{\nu^n d\nu}{\sqrt{1 + 2D\nu + \left(D^2 - \frac{1}{C^2}\right)\nu^2}} = \frac{1}{n + 1} I_{3,n}' \qquad \text{(A8)}$$

Use can be made of the recursion formula

$$I_{3,n}' = 2\int_0^{\frac{C}{1-CD}} \frac{\nu^n d\nu}{\sqrt{1 + 2D\nu + \left(D^2 - \frac{1}{C^2}\right)\nu^2}}$$

$$= \frac{1}{n}\frac{C^2}{1 - C^2D^2}\left[(2n - 1)DI_{3,n-1}' + (n - 1)I_{3,n-2}'\right] \qquad (n \geq 2) \quad (A9)$$

and of

$$I_{3,0}' = \frac{2C}{\sqrt{1 - C^2D^2}}\left(\frac{\pi}{2} + \sin^{-1}CD\right) \qquad (n = 0) \qquad (A10)$$

$$I_{3,1}' = \frac{C^2}{1 - C^2D^2}\left(2 + DI_{3,0}'\right) \qquad (n = 1) \qquad (A11)$$

Supersonic-Leading-Edge Wing

The spanwise integral of E_{mn} is (with the cotangent of the leading-edge sweep angle designated by C in the present paper rather than by λ as in ref. 4)

$$\bar{E}_{mn} = 2R.P.\int_0^{\frac{C}{1-CD}} 2^{m+n+1}\nu^m(1 + D\nu)^n\sqrt{1 + 2D\nu + (D^2 - \beta^2)\nu^2}\, d\nu \qquad (A12)$$

where R.P. means the real part of the quantity to follow. The quantities $\bar{E}_{mn}$ are seen to equal 2^{m+n+1} times $I_{2,n}{}^m$ of equation (A5), provided that C is replaced by $1/\beta$ in the integrand and in the upper limit of equation (A5); thus, $\bar{E}_{mn}$ can be evaluated by use of equations (A3) and (A6) once the substitution of $1/\beta$ for C is made.

The spanwise integral of F_{mn}^{e} is

$$\bar{F}_{mn}^{e} = 2R.P.\int_{0}^{\frac{C}{1-CD}} 2^{e+m+n}\left\{(\beta^2 C\nu)^e(1+D\nu)^m\left[C+(CD+1)\nu\right]^n \cos^{-1}\frac{1+(D+\beta^2C)\nu}{\beta\left[C+(CD+1)\nu\right]} + \right.$$

$$\left.(-\beta^2C\nu)^e(1+D\nu)^m\left[C+(CD-1)\nu\right]^n\cos^{-1}\frac{1+(D-\beta^2C)\nu}{\beta\left[C+(CD-1)\nu\right]}\right\}d\nu \qquad (A13)$$

Through integration by parts, it can be determined that

$$\begin{Bmatrix}K_{1,n}'\\K_{1,n}''\end{Bmatrix} = R.P.\int_{0}^{\frac{C}{1-CD}}\left[C+(CD\pm1)\nu\right]^n\cos^{-1}\frac{1+(D\pm\beta^2C)\nu}{\beta\left[C+(CD\pm1)\nu\right]}\,d\nu$$

$$= \frac{\mp C^{n+1}\cos^{-1}(1/\beta C)}{(n+1)(1\pm CD)} + \frac{\sigma}{(n+1)(1\pm CD)}\begin{Bmatrix}K_{2,n}'\\K_{2,n}''\end{Bmatrix} \qquad (A14)$$

where the upper quantity $K_{1,n}'$ is associated with $K_{2,n}'$ and the upper of the alternate signs $\pm$ or $\mp$, and the lower quantity $K_{1,n}''$ with $K_{2,n}''$ and the lower of the alternate signs. The quantities $K_{2,n}'$ and $K_{2,n}''$ can be determined by the recursion formula

$$\begin{Bmatrix}K_{2,n}'\\K_{2,n}''\end{Bmatrix} = R.P.\int_{0}^{\frac{C}{1-CD}}\frac{\left[C+(CD\pm1)\nu\right]^n d\nu}{\sqrt{1+2D\nu+(D^2-\beta^2)\nu^2}}$$

$$= \frac{1}{n(\beta^2-D^2)}\left[C^{n-1}(CD\pm1)+(2n-1)(\beta^2C\pm D)\begin{Bmatrix}K_{2,n-1}'\\K_{2,n-1}''\end{Bmatrix} - (n-1)\sigma\begin{Bmatrix}K_{2,n-2}'\\K_{2,n-2}''\end{Bmatrix}\right] \qquad (n\geq 1) \qquad (A15)$$

and

$$\begin{Bmatrix} K_{2,0}' \\ K_{2,0}'' \end{Bmatrix} = \frac{1}{\sqrt{\beta^2 - D^2}}\left(\frac{\pi}{2} + \sin^{-1}\frac{D}{\beta}\right) \qquad (n = 0) \tag{A16}$$

The quantities $\bar{F}_{mn}^{e}$ (needed for forces and moments to the third power of the frequency) can be expressed as

$$\left.\begin{aligned}
\bar{F}_{0n}^{0} &= 2^{n+1}\left(K_{1,n}' + K_{1,n}''\right) \\
\bar{F}_{1n}^{0} &= 2^{n+2}\left(\frac{K_{1,n}' + DK_{1,n+1}'}{1 + CD} + \frac{K_{1,n}'' - DK_{1,n+1}''}{1 - CD}\right) \\
\bar{F}_{2n}^{0} &= 2^{n+3}\left[\frac{1}{(1 + CD)^2}\left(K_{1,n}' + 2DK_{1,n+1}' + D^2K_{1,n+2}'\right) + \right. \\
&\qquad \left. \frac{1}{(1 - CD)^2}\left(K_{1,n}'' - 2DK_{1,n+1}'' + D^2K_{1,n+2}''\right)\right] \\
\bar{F}_{0n}^{1} &= 2^{n+2}\beta^2C\left(\frac{K_{1,n+1}' - CK_{1,n}'}{1 + CD} + \frac{K_{1,n+1}'' - CK_{1,n}'}{1 - CD}\right) \\
\bar{F}_{1n}^{1} &= 2^{n+3}\beta^2C\left\{\frac{1}{(1 + CD)^2}\left[-CK_{1,n}' + (1 - CD)K_{1,n+1}' + DK_{1,n+2}'\right] + \right. \\
&\qquad \left. \frac{1}{(1 - CD)^2}\left[-CK_{1,n}'' + (1 + CD)K_{1,n+1}'' - DK_{1,n+2}''\right]\right\}
\end{aligned}\right\} \tag{A17}$$

The remaining required integral is

$$I_{4,n} = 2R.P.\int_0^{\frac{C}{1-CD}} \nu^n \cosh^{-1}\frac{1+D\nu}{\beta\nu}\,d\nu$$

$$= 2\int_0^{\frac{1}{\beta-D}} \nu^n \cosh^{-1}\frac{1+D\nu}{\beta\nu}\,d\nu \qquad (A18)$$

which, after integration by parts, is the same as $I_{3,n}$ if C is replaced by $1/\beta$ in equation (A8). Thus,

$$I_{4,n} = \frac{1}{n+1} I_{4,n}' \qquad (A19)$$

and

$$I_{4,0}' = \frac{2}{\sqrt{\beta^2 - D^2}}\left(\frac{\pi}{2} + \sin^{-1}\frac{D}{\beta}\right) \qquad (n = 0) \qquad (A20)$$

$$I_{4,1}' = \frac{1}{\beta^2 - D^2}\left(2 + DI_{4,0}'\right) \qquad (n = 1) \qquad (A21)$$

$$I_{4,n}' = \frac{1}{n(\beta^2 - D^2)}\left[(2n-1)DI_{4,n-1}' + (n-1)I_{4,n-2}'\right] \qquad (n \geq 2) \qquad (A22)$$

The spanwise integrals of the quantities G_{mn} of reference 4 can now be expressed as follows:

$$\left.\begin{aligned}
\bar{G}_{01} &= \frac{1}{3}\left(\bar{E}_{02} - \beta^2\bar{E}_{20}\right) \\
\bar{G}_{02} &= \frac{1}{4}\bar{E}_{03} - \frac{1}{8}\bar{E}_{21} - 2\beta^4 I_{4,4} \\
\bar{G}_{03} &= \frac{1}{15}\left(3\bar{E}_{04} - \beta^2\bar{E}_{22} - 2\beta^4\bar{E}_{40}\right) \\
\bar{G}_{20} &= \frac{1}{2}\bar{E}_{21} - 8\beta^2 I_{4,4} \\
\bar{G}_{21} &= \frac{1}{3}\left(\bar{E}_{22} - \beta^2\bar{E}_{40}\right)
\end{aligned}\right\} \qquad \text{(A23)}$$

The spanwise integrals of the quantities H_{mn}^{e} of reference 4 can also be expressed as follows:

$$\bar{H}_{01}{}^{0} = \frac{1}{2c}\bar{F}_{02}{}^{0} - \frac{4}{c}\sqrt{\sigma} I_{4,2} \qquad \text{(A24a)}$$

$$\bar{H}_{02}{}^{0} = \frac{1}{3c}\bar{F}_{03}{}^{0} - \frac{4}{3}\sqrt{\sigma}\,\bar{E}_{20} \qquad \text{(A24b)}$$

$$\bar{H}_{03}{}^{0} = \frac{1}{4c}\bar{F}_{04}{}^{0} - \frac{4}{c}\sqrt{\sigma}\left[\frac{3c^2}{16}\bar{E}_{21} + (3\sigma + 5) I_{4,4}\right] \qquad \text{(A24c)}$$

$$\bar{H}_{04}{}^{0} = \frac{1}{5c}\bar{F}_{05}{}^{0} - \frac{8}{15}\sqrt{\sigma}\left[(2\sigma + 5)\bar{E}_{40} + c^2\bar{E}_{22}\right] \qquad \text{(A24d)}$$

$$\bar{H}_{11}{}^{0} = \frac{-1}{6c^2}\bar{F}_{03}{}^{0} + \frac{1}{2c}\bar{F}_{12}{}^{0} - \frac{\sqrt{\sigma}}{3c}\bar{E}_{20} \qquad \text{(A24e)}$$

$$\bar{H}_{12}^{0} = \frac{-1}{12c^2}\bar{F}_{04}^{0} + \frac{1}{3c}\bar{F}_{13}^{0} - \frac{4\sqrt{\sigma}}{3c^2}\left[\frac{5c^2}{16}\bar{E}_{21} + (5\sigma + 3)I_{4,4}\right] \tag{A24f}$$

$$\bar{H}_{13}^{0} = \frac{-1}{20c^2}\bar{F}_{05}^{0} + \frac{1}{4c}\bar{F}_{14}^{0} - \frac{\sqrt{\sigma}}{30c}\left[(22\sigma + 25)\bar{E}_{40} + 11c^2\bar{E}_{22}\right] \tag{A24g}$$

$$\bar{H}_{21}^{0} = \frac{1}{12c^3}\bar{F}_{04}^{0} - \frac{1}{3c^2}\bar{F}_{13}^{0} + \frac{1}{2c}\bar{F}_{22}^{0} - \frac{4\sqrt{\sigma}}{3c^3}\left[\frac{c^2}{16}\bar{E}_{21} + (\sigma + 3)I_{4,4}\right] \tag{A24h}$$

$$\bar{H}_{22}^{0} = \frac{1}{30c^3}\bar{F}_{05}^{0} - \frac{1}{6c^2}\bar{F}_{14}^{0} + \frac{1}{3c}\bar{F}_{23}^{0} - \frac{\sqrt{\sigma}}{15c^2}\left[3c^2E_{22} + (6\sigma + 5)\bar{E}_{40}\right] \tag{A24i}$$

$$\bar{H}_{01}^{1} = \frac{1}{2c}\bar{F}_{02}^{1} - \beta^2 c\sqrt{\sigma}\,\bar{E}_{20} \tag{A24j}$$

$$\bar{H}_{11}^{1} = \frac{-\beta^2}{6c}\bar{F}_{04}^{0} + \frac{2\beta^2}{3}\bar{F}_{13}^{0} - \frac{\beta^2 c}{2}\bar{F}_{22}^{0} - \frac{\beta^2\sqrt{\sigma}}{3c}\left(c^2\bar{E}_{21} + 16\sigma I_{4,4}\right) \tag{A24k}$$

$$\bar{H}_{03}^{1} = \frac{1}{4c}\bar{F}_{04}^{1} - \frac{\beta^2}{6}c\sqrt{\sigma}\left[c^2\bar{E}_{22} + (2\sigma + 11)\bar{E}_{40}\right] \tag{A24l}$$

A few differences of exponents and multiplying factors can be noted between the equations for certain of the $\bar{G}_{mn}$ and $\bar{H}_{mn}^{e}$ above and the section quantities G_{mn} and H_{mn}^{e} of reference 4. The printing errors of reference 4 have been corrected in two errata notices; they were present in G_{03}, G_{20}, H_{21}^{0}, H_{11}^{1}, and H_{03}^{1}.

REFERENCES

1. Miles, John W.: On Harmonic Motion of Wide Delta Airfoils at Supersonic Speeds. TM RRB-36, U. S. Naval Ordnance Test Station, Inyokern, Calif., Feb. 9, 1950.

2. Froehlich, Jack E.: Nonstationary Motion of Purely Supersonic Wings. Jour. Aero. Sci., vol. 18, no. 5, May 1951, pp. 298-310.

3. Watkins, Charles E., and Berman, Julian H.: Air Forces and Moments on Triangular and Related Wings With Subsonic Leading Edges Oscillating in Supersonic Potential Flow. NACA Rep. 1099, 1952.

4. Nelson, Herbert C.: Lift and Moment on Oscillating Triangular and Related Wings With Supersonic Edges. NACA TN 2494, 1951.

5. Malvestuto, Frank S., Jr., and Margolis, Kenneth: Theoretical Stability Derivatives of Thin Sweptback Wings Tapered to a Point With Sweptback or Sweptforward Trailing Edges for a Limited Range of Supersonic Speeds. NACA Rep. 971, 1950. (Supersedes NACA TN 1761.)

6. Harmon, Sidney M., and Jeffreys, Isabella: Theoretical Lift and Damping in Roll of Thin Wings With Arbitrary Sweep and Taper at Supersonic Speeds - Supersonic Leading and Trailing Edges. NACA TN 2114, 1950.

7. Martin, John C., Margolis, Kenneth, and Jeffreys, Isabella: Calculation of Lift and Pitching Moments Due to Angle of Attack and Steady Pitching Velocity at Supersonic Speeds for Thin Sweptback Tapered Wings With Streamwise Tips and Supersonic Leading and Trailing Edges. NACA TN 2699, 1952.

8. Cole, Isabella J., and Margolis, Kenneth: Lift and Pitching Moment at Supersonic Speeds Due to Constant Vertical Acceleration for Thin Sweptback Tapered Wings With Streamwise Tips - Supersonic Leading and Trailing Edges. NACA TN 3196, 1954.

TABLE I

TOTAL LIFT AND MOMENT FLUTTER COEFFICIENTS FOR AN ARROWHEAD WING WITH $\mu_0 = 0$, $\Lambda = 45^\circ$, AND $\Lambda_{TE} = 0^\circ$ AT VARIOUS MACH NUMBERS

M	$\bar{L}_1/c$	$\bar{L}_2/c$	$\bar{L}_3/c$	$\bar{L}_4/c$	$\bar{M}_1/c$	$\bar{M}_2/c$	$\bar{M}_3/c$	$\bar{M}_4/c$
1.05687	$2.8466 - 76.050k^2 + 1740.98k^4$	$1.4044(1/k) - 15.073k + 394.01k^3$	$1.4044(1/k^2) - 9.8148 + 291.58k^2$	$-0.4339(1/k) + 52.872k - 1326.32k^3$	$6.2700 - 132.25k^2 + 3156.12k^4$	$1.8726(1/k) - 24.1167k + 962.41k^3$	$1.8726(1/k^2) - 15.704 + 810.93k^2$	$-2.6509(1/k) + 93.62k - 2401.5k^3$
1.15282	$1.5083 - 10.234k^2 + 38.799k^4$	$1.2480(1/k) - 4.2036k + 22.209k^3$	$1.2480(1/k^2) - 2.0420 + 12.279k^2$	$0.4084(1/k) + 5.3616k - 22.2784k^3$	$2.2624 - 17.0575k^2 + 74.932k^4$	$1.6640(1/k) - 6.7258k + 30.288k^3$	$1.6640(1/k^2) - 3.2670 + 16.959k^2$	$0.6125(1/k) + 8.9365k - 42.791k^3$
1.29268	$0.8999 - 2.5228k^2 + 3.7767k^4$	$1.0967(1/k) - 1.6635k + 3.3096k^3$	$1.0967(1/k^2) - 0.6268 + 1.3725k^2$	$0.6385(1/k) + 0.9888k - 1.6115k^3$	$1.3498 - 4.2049k^2 + 6.6088k^4$	$1.4623(1/k) - 2.6614k + 5.6734k^3$	$1.4623(1/k^2) - 1.0028 + 2.3524k^2$	$0.9578(1/k) + 1.6481k - 2.8205k^3$
1.41421	$0.6667 - 1.2000k^2 + 1.0865k^4$	$1.0000(1/k) - 1.0000k + 1.2222k^3$	$1.0000(1/k^2) - 0.3333 + 0.4213k^2$	$0.6667(1/k) + 0.4000k - 0.3889k^3$	$1.0000 - 2.0000k^2 + 1.9013k^4$	$1.3333(1/k) - 1.6000k + 2.9095k^3$	$1.3333(1/k^2) - 0.5333 + 0.7226k^2$	$1.0000(1/k) + 0.6667k + 0.6763k^3$

TABLE II

TOTAL LIFT AND MOMENT FLUTTER COEFFICIENTS FOR ARROWHEAD WINGS WITH $\mu_0 = 0$ AND $\Lambda_{TE} = 0^\circ$ FOR VARIOUS LEADING-EDGE SWEEP ANGLES

(a) M = 1.15282

Λ, deg	$\bar{L}_1/c$	$\bar{L}_2/c$	$\bar{L}_3/c$	$\bar{L}_4/c$	$\bar{M}_1/c$	$\bar{M}_2/c$	$\bar{M}_3/c$	$\bar{M}_4/c$
≤ 29.8	$3.5329 - 27.3708k^2 + 117.893k^4$	$1.7434(1/k) - 10.7075k + 60.5701k^3$	$1.7434(1/k^2) - 7.1739 + 42.3383k^2$	$-1.2083(1/k) + 18.8519k - 83.3385k^3$	$5.3192 - 45.6515k^2 + 204.605k^4$	$2.3246(1/k) - 17.1400k + 286.320k^3$	$2.3246(1/k^2) - 11.4839 + 255.051k^2$	$-1.8269(1/k) + 31.444k - 142.481k^3$
45	$1.5083 - 10.234k^2 + 38.799k^4$	$1.2480(1/k) - 4.2036k + 22.209k^3$	$1.2480(1/k^2) - 2.0420 + 12.279k^2$	$0.4084(1/k) + 5.3616k - 22.2784k^3$	$2.2624 - 17.0575k^2 + 74.932k^4$	$1.6640(1/k) - 6.7258k + 30.288k^3$	$1.6640(1/k^2) - 3.2670 + 16.959k^2$	$0.61251(1/k) + 8.9365k - 42.791k^3$
59.6	$0.39601 - 2.5950k^2 + 10.059k^4$	$0.83745(1/k) - 1.1340k + 5.3503k^3$	$0.83745(1/k^2) - 0.22268 + 1.8948k^2$	$1.0426(1/k) + 0.73535k - 4.0778k^3$	$0.59400 - 4.3247k^2 + 17.604k^4$	$1.1166(1/k) - 1.8145k + 9.1721k^3$	$1.1166(1/k^2) - 0.34917 + 3.2425k^2$	$1.5640(1/k) + 1.2253k - 7.1372k^3$
73.2	$-0.08533 - 0.27792k^2 + 1.5452k^4$	$0.45725(1/k) - 0.09640k + 0.58165k^3$	$0.45725(1/k^2) - 0.053081 + 0.12981k^2$	$0.94541(1/k) + 0.03135k - 0.80443k^3$	$-0.12800 - 0.46320k^2 + 3.6785k^4$	$0.60965(1/k) - 0.15424k + 0.9972k^3$	$0.60965(1/k^2) - 0.08493 + 0.22265k^2$	$1.4181(1/k) + 0.05229k - 2.4035k^3$

TABLE II.- Concluded

TOTAL LIFT AND MOMENT FLUTTER COEFFICIENTS FOR ARROWHEAD WINGS WITH $\mu_0 = 0$ AND $\Lambda_{TE} = 0^\circ$ FOR VARIOUS LEADING-EDGE SWEEP ANGLES

(b) $M \approx 1.30$

Λ, deg	M	$\bar{L}_1/C$	$\bar{L}_2/C$	$\bar{L}_3/C$	$\bar{L}_4/C$	$\bar{M}_1/C$	$\bar{M}_2/C$	$\bar{M}_3/C$	$\bar{M}_4/C$
≤39.7	1.300	$1.1632 - 3.2199k^2 + 4.6230k^4$	$1.2039(1/k) - 2.1366k + 4.1122k^3$	$1.2039(1/k^2) - 0.9742 + 1.9743k^2$	$0.4420(1/k) + 1.5172k - 2.2751k^3$	$1.7447 - 5.3410k^2 + 8.0904k^4$	$1.6051(1/k) - 3.4651k + 7.0502k^3$	$1.6051(1/k^2) - 1.5792 + 3.3854k^2$	$0.6628(1/k) + 2.5031k - 3.9811k^3$
45	1.293	$0.8999 - 2.5228k^2 + 3.7767k^4$	$1.0967(1/k) - 1.6635k + 3.3096k^3$	$1.0967(1/k^2) - 0.6268 + 1.3725k^2$	$0.6385(1/k) + 0.9888k - 1.6115k^3$	$1.3498 - 4.2049k^2 + 6.6088k^4$	$1.4623(1/k) - 2.6614k + 5.6734k^3$	$1.4623(1/k^2) - 1.0028 + 2.3524k^2$	$0.9578(1/k) + 1.6481k - 2.8205k^3$
50	1.308	$0.6258 - 1.6273k^2 + 2.2450k^4$	$0.9760(1/k) - 1.1194k + 2.0979k^3$	$0.9760(1/k^2) - 0.30412 + 0.6547k^2$	$0.7962(1/k) + 0.4727k - 0.7547k^3$	$0.9387 - 2.8563k^2 + 3.9285k^4$	$1.3012(1/k) - 1.7911k + 3.4960k^3$	$1.3012(1/k^2) - 0.4865 + 1.0998k^2$	$1.1943(1/k) + 1.0407k - 1.3208k^3$
60	1.323	$0.22231 - 0.6072k^2 + 0.7617k^4$	$0.7488(1/k) - 0.4329k + 0.7252k^3$	$0.7488(1/k^2) + 0.00467 + 0.04961k^2$	$0.9660(1/k) + 0.01110k - 0.08085k^3$	$0.3335 - 1.0120k^2 + 1.3332k^4$	$0.9984(1/k) - 0.6927k + 1.2435k^3$	$0.9984(1/k^2) + 0.00742 + 0.08526k^2$	$1.4490(1/k) + 0.01853k - 0.1417k^3$

TABLE III

TOTAL LIFT AND MOMENT FLUTTER COEFFICIENTS FOR ARROWHEAD WINGS WITH $\mu_0 = 0$, $\Lambda = 45^\circ$, AND $M = 1.50$ FOR VARIOUS TRAILING-EDGE SWEEP ANGLES

Λ_{TE}, deg	$\bar{L}_1/c$	$\bar{L}_2/c$	$\bar{L}_3/c$	$\bar{L}_4/c$	$\bar{M}_1/c$	$\bar{M}_2/c$	$\bar{M}_3/c$	$\bar{M}_4/c$
20	$1.2179 - 2.3530k^2$	$1.5683(1/k) - 1.8934k$	$1.5683(1/k^2) - 0.4380$	$1.4094(1/k) + 0.5527k$	$2.5533 - 5.2364k^2$	$2.8391(1/k) - 4.1086k$	$2.8391(1/k^2) - 0.9114$	$2.7595(1/k) + 1.2060k$
10	$0.7113 - 1.1354k^2$	$1.1365(1/k) - 1.0089k$	$1.1365(1/k^2) - 0.2524$	$0.9468(1/k) + 0.2788k$	$1.2246 - 2.1109k^2$	$1.7165(1/k) - 1.8191k$	$1.7165(1/k^2) - 0.4502$	$1.5703(1/k) + 0.5162k$
0	$0.4771 - 0.6871k^2 + 0.4844k^4$	$0.8944(1/k) - 0.6441k + 0.6182k^3$	$0.8944(1/k^2) - 0.1671 + 0.1598k^2$	$0.7155(1/k) + 0.1739k - 0.1316k^3$	$0.7156 - 1.1452k^2 + 0.8478k^4$	$1.1926(1/k) - 1.0306k + 1.0598k^3$	$1.1926(1/k^2) - 0.2674 + 0.2739k^2$	$1.0733(1/k) + 0.2898k - 0.2303k^2$
-10	$0.3431 - 0.4663k^2$	$0.7331(1/k) - 0.4508k$	$0.7331(1/k^2) - 0.1191$	$0.5717(1/k) + 0.1175k$	$0.4629 - 0.7237k^2$	$0.8882(1/k) - 0.6636k$	$0.8882(1/k^2) - 0.1759$	$0.7994(1/k) + 0.1827k$

TABLE IV

RELATION BETWEEN FLUTTER AND STABILITY COEFFICIENT NOTATION

Flutter coefficients		Stability coefficients as in ref. 5
Present paper (a)	Ref. 1 (for delta wing only)	(b)
$f_a \frac{\bar{L}_1}{C}$	$-\frac{1}{k^2} R_{L_h} \tan\theta$	$-\frac{1}{6} C_{L_{\dot{\alpha}}}'$
$f_a k \frac{\bar{L}_2}{C}$	$-\frac{1}{k} I_{L_h} \tan\theta$	$\frac{1}{4} C_{L_\alpha}'$
$f_a k^2 \frac{\bar{L}_3}{C}$	$\left[R_{L_\alpha} + \left(a - \frac{1}{3}\right) R_{L_h}\right] \tan\theta$	$\frac{1}{4} C_{L_\alpha}'$
$f_a k \frac{\bar{L}_4}{C}$	$\frac{1}{k}\left[I_{L_\alpha} + \left(a - \frac{1}{3}\right) I_{L_h}\right] \tan\theta$	$\frac{1}{6}\left(C_{L_q}' + C_{L_{\dot{\alpha}}}'\right)$
$f_a \frac{\bar{M}_1}{C}$	$\frac{1}{k^2}\left[R_{M_h} + \left(a - \frac{1}{3}\right) R_{L_h}\right] \tan\theta$	$\frac{2}{9} C_{m_{\dot{\alpha}}}'$
$f_a k \frac{\bar{M}_2}{C}$	$\frac{1}{k}\left[I_{M_h} + \left(a - \frac{1}{3}\right) I_{L_h}\right] \tan\theta$	$-\frac{1}{3} C_{m_\alpha}'$
$f_a k^2 \frac{\bar{M}_3}{C}$	$-\left[R_{M_\alpha} + \left(a - \frac{1}{3}\right)\left(R_{L_\alpha} + R_{M_h}\right) + \left(a - \frac{1}{3}\right)^2 R_{L_h}\right] \tan\theta$	$-\frac{1}{3} C_{m_\alpha}'$
$f_a k \frac{\bar{M}_4}{C}$	$-\frac{1}{k}\left[I_{M_\alpha} + \left(a - \frac{1}{3}\right)\left(I_{L_\alpha} + I_{M_h}\right) + \left(a - \frac{1}{3}\right)^2 I_{L_h}\right] \tan\theta$	$-\frac{2}{9}\left(C_{m_q}' + C_{m_{\dot{\alpha}}}'\right)$

[a]The area factor $f_a = 1 - CD$ is unity for the delta wing.

[b]The fractions in this column would be different, in general, for nonarrowhead wings.

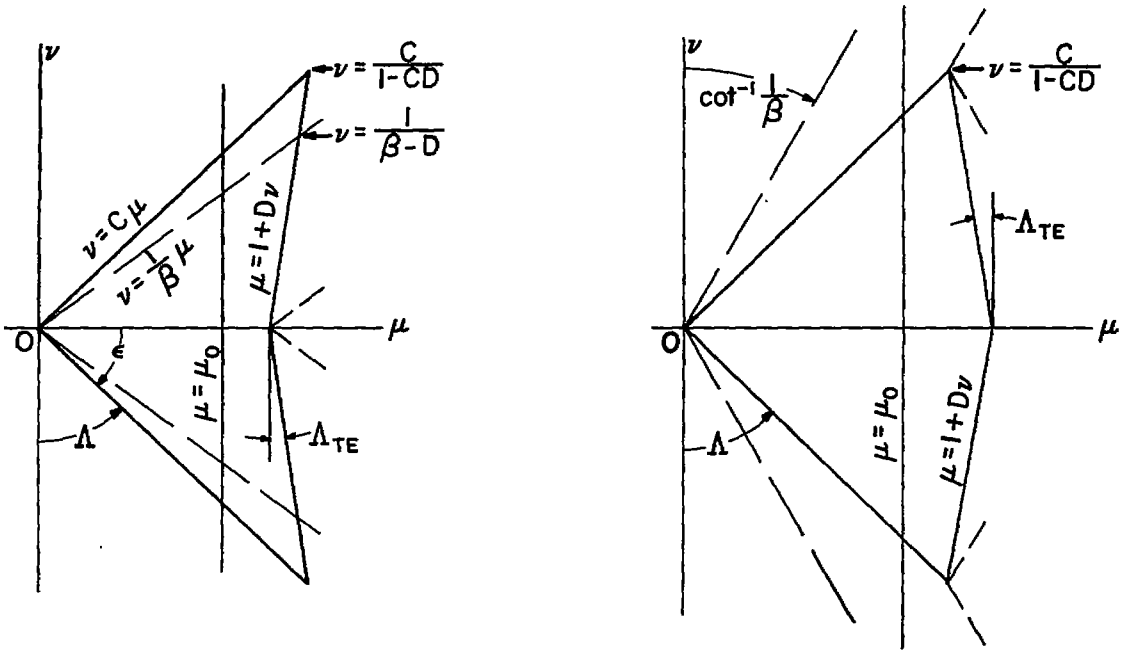

(a) Projection of plan forms on $\mu\nu$-plane. $C = \cot \Lambda$; $D = \tan \Lambda_{TE}$.

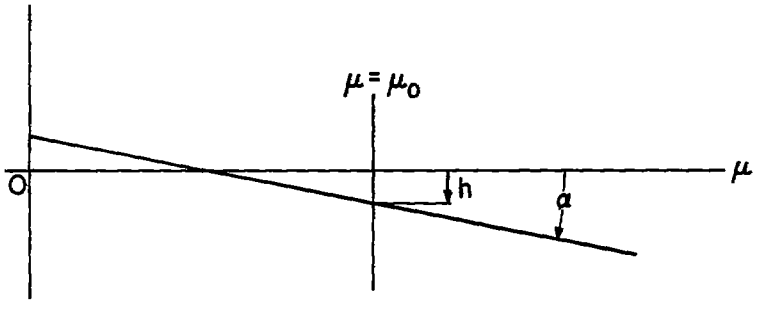

(b) Section $\nu = 0$.

Figure 1.- Sketch illustrating two arrowhead plan forms, coordinate system, and the two degrees of freedom h and α.

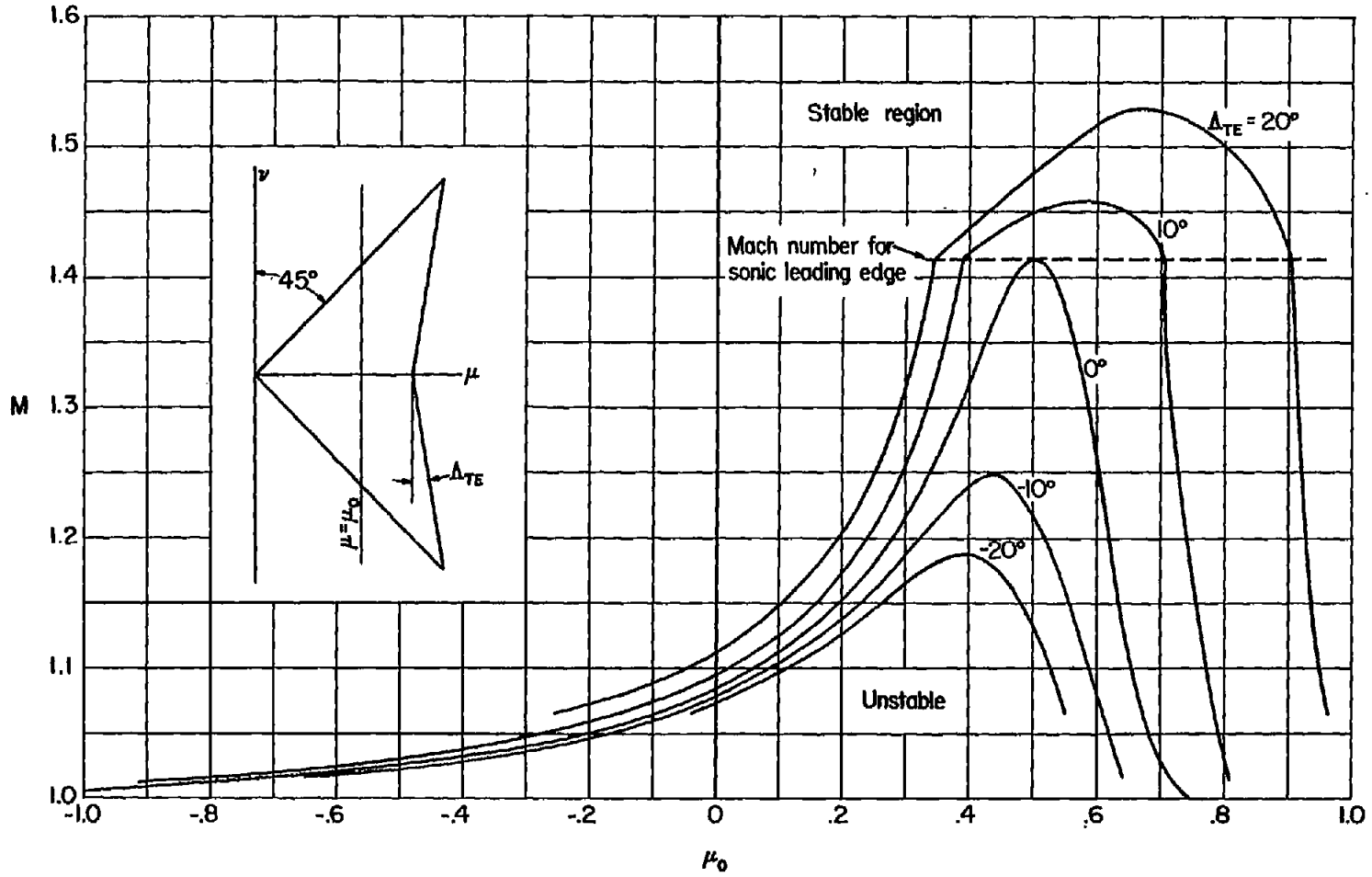

Figure 2.- Curves showing ranges of Mach number M and axis of rotation μ_0 for which the aerodynamic pitching moment vanishes for slow oscillations of arrowhead wings with leading-edge sweepback of 45° and various trailing-edge sweep angles. Curves are ended at M for which trailing edge is sonic.

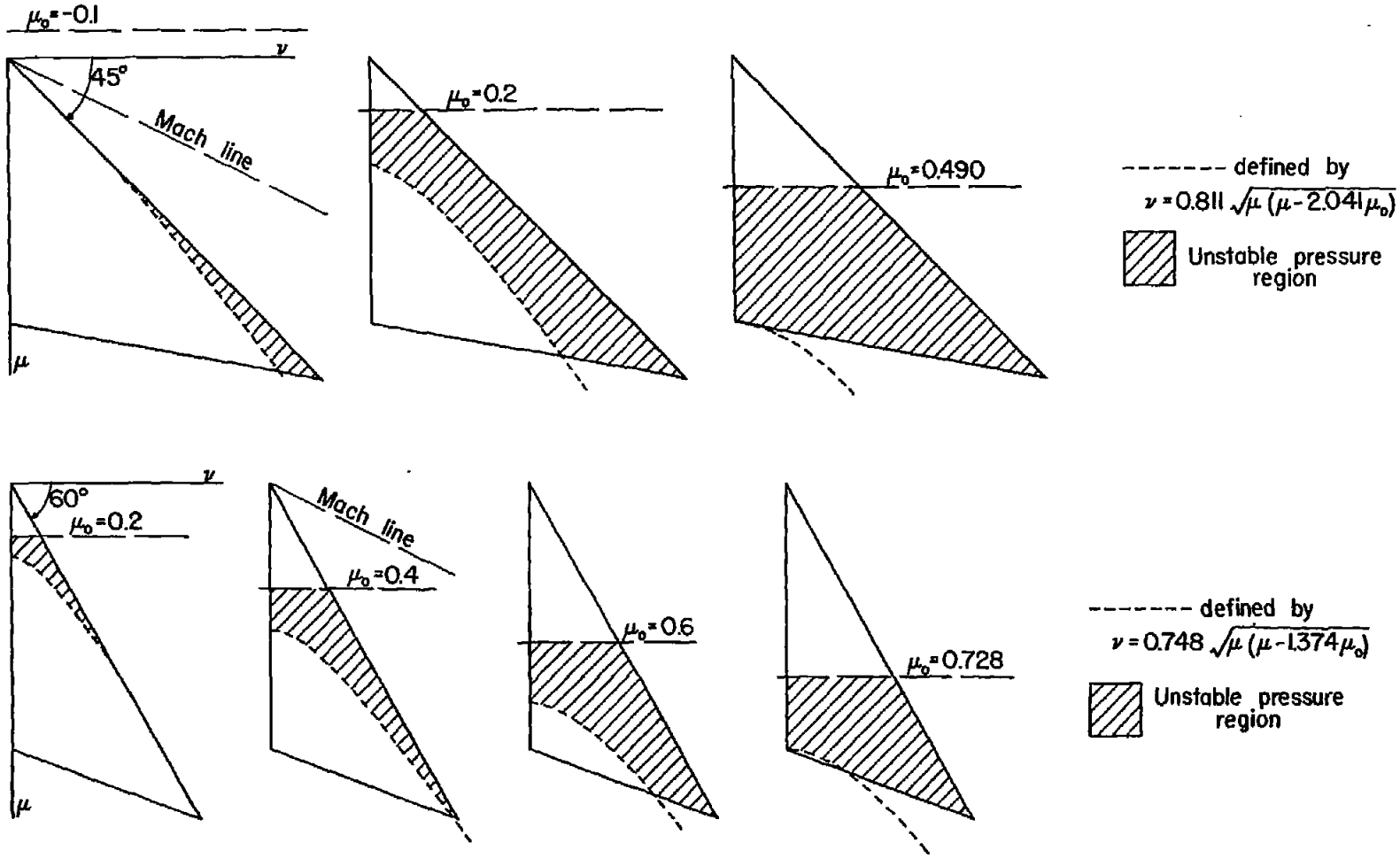

Figure 3.- Sketch showing regions having a pressure which contributes to pitching instability for slow oscillations of arrowhead wings with leading-edge sweep angles of 45° and 60°, a Mach number of 10/9, and with various locations of pitch axis μ_0.

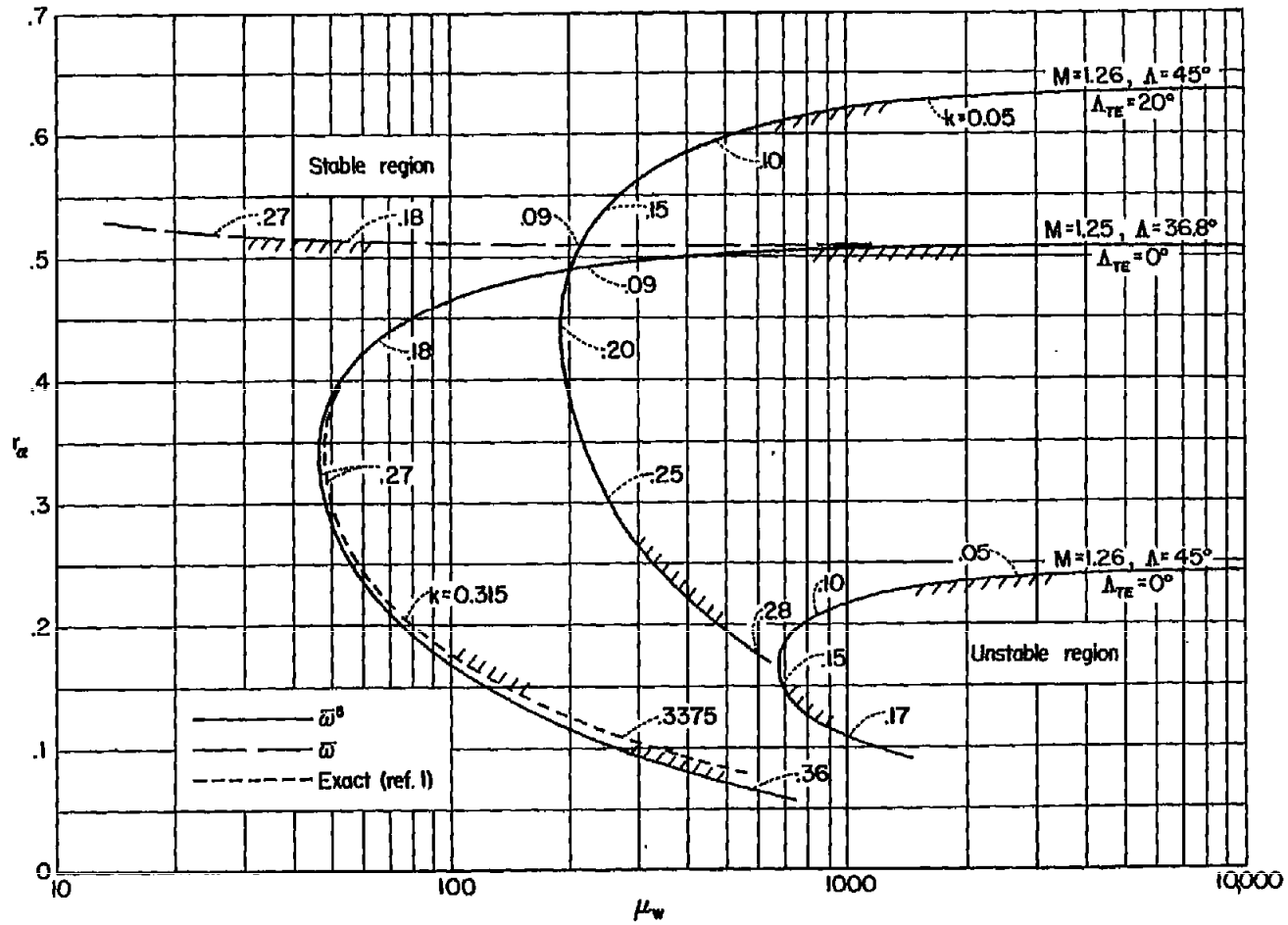

Figure 4.- Curves separating stable and unstable regions of radius of gyration r_α and mass ratio of wing μ_w for three arrowhead-wing plan forms with two longitudinal degrees of freedom, pitch and vertical translation, at $M \approx 1.25$ with $\mu_0 = 0.5$.

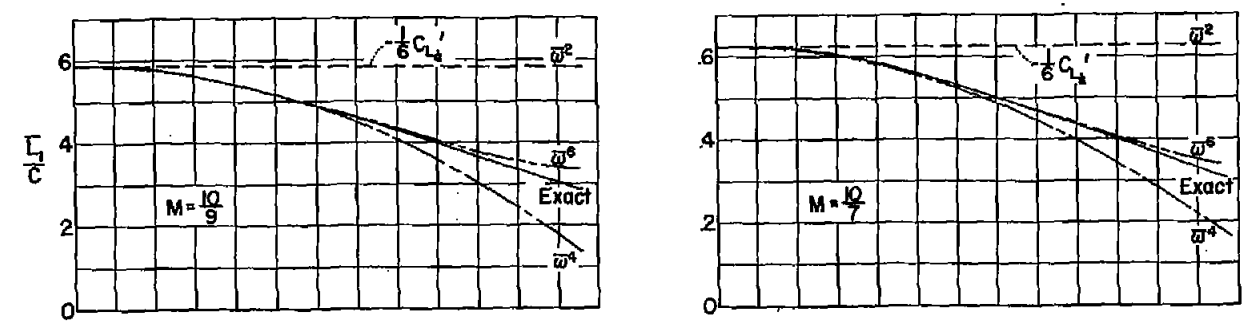

(a) Real part of lift-curve slope associated with vertical translation of wing.

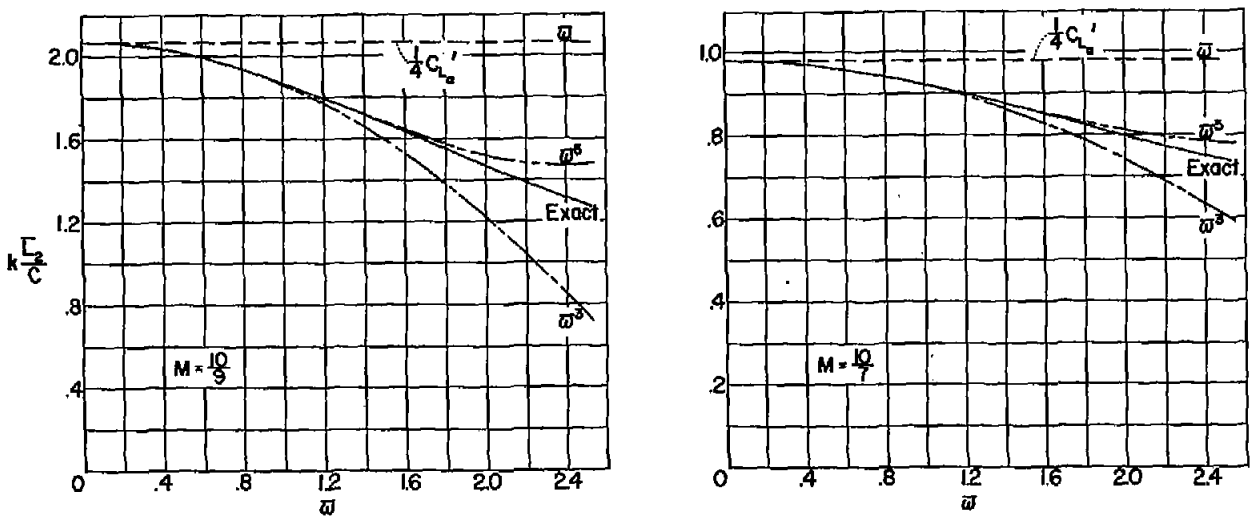

(b) Imaginary part of lift-curve slope associated with vertical translation of wing.

Figure 5.- Comparison of lift- and moment-curve slopes obtained from exact and approximate theory as a function of frequency parameter for sonic- and supersonic-leading-edge delta wings with $\mu_0 = 0.5$ for $M = 10/9$ and $10/7$. The power of $\bar{\omega}$ required to produce each approximate curve is indicated.

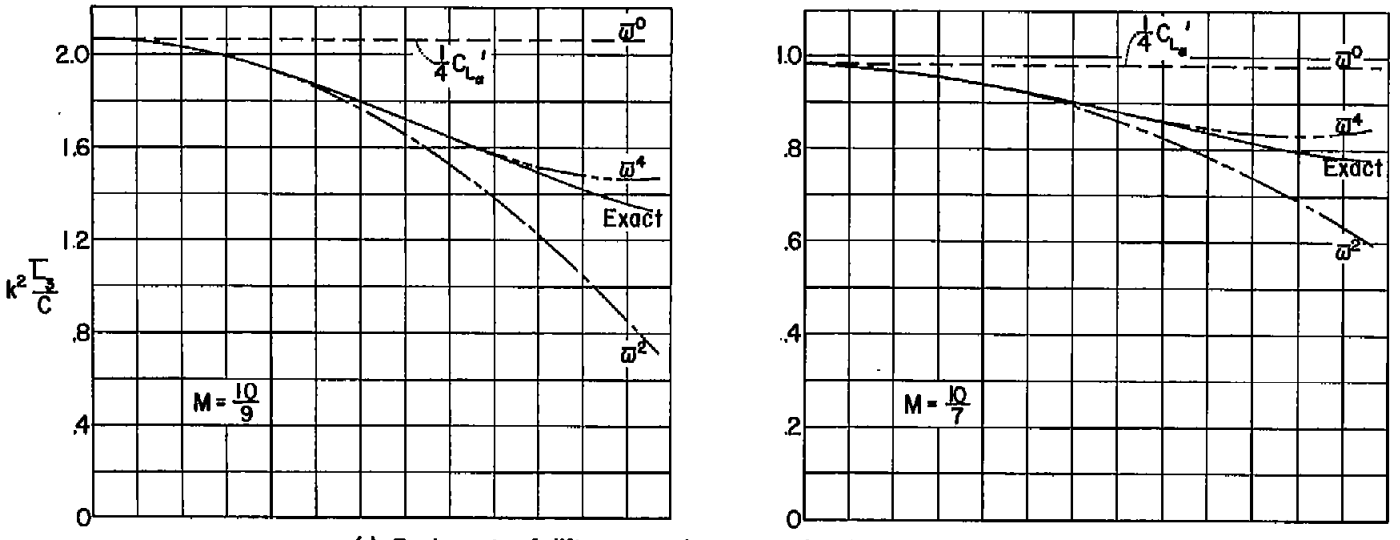

(c) Real part of lift-curve slope associated with pitching of wing.

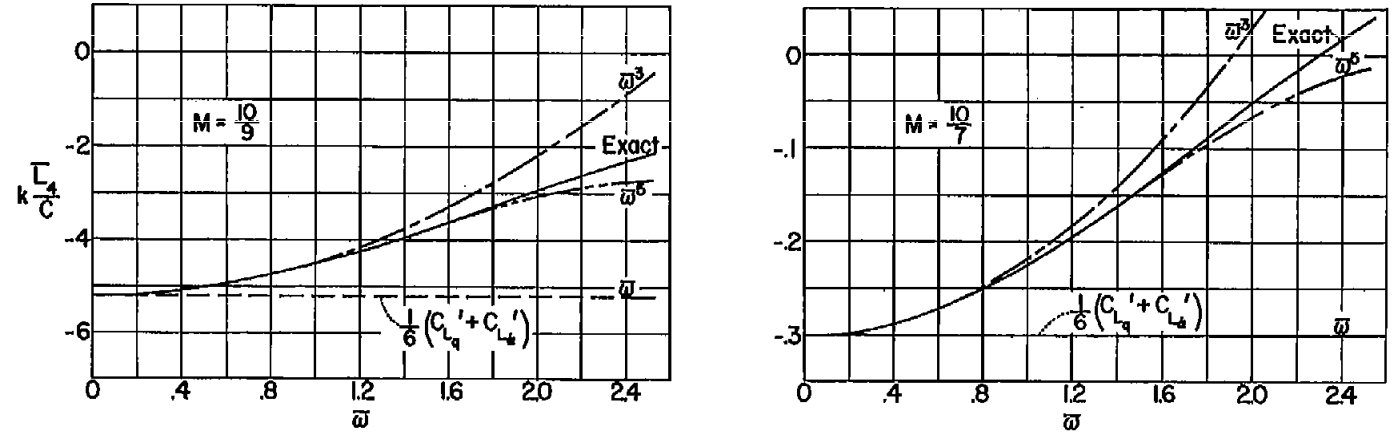

(d) Imaginary part of lift-curve slope associated with pitching of wing.

Figure 5.- Continued.

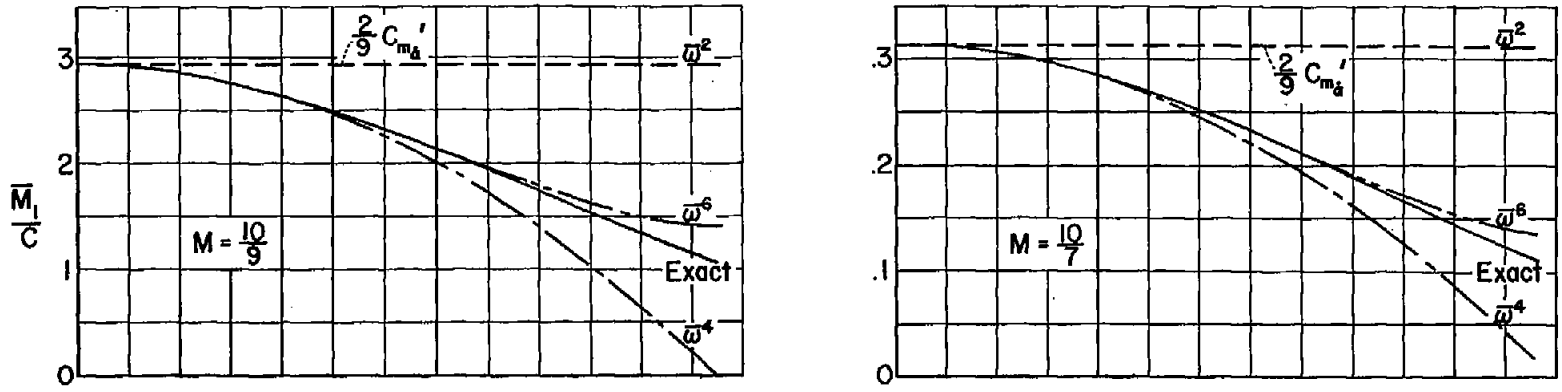

(e) Real part of moment-curve slope associated with vertical translation of wing.

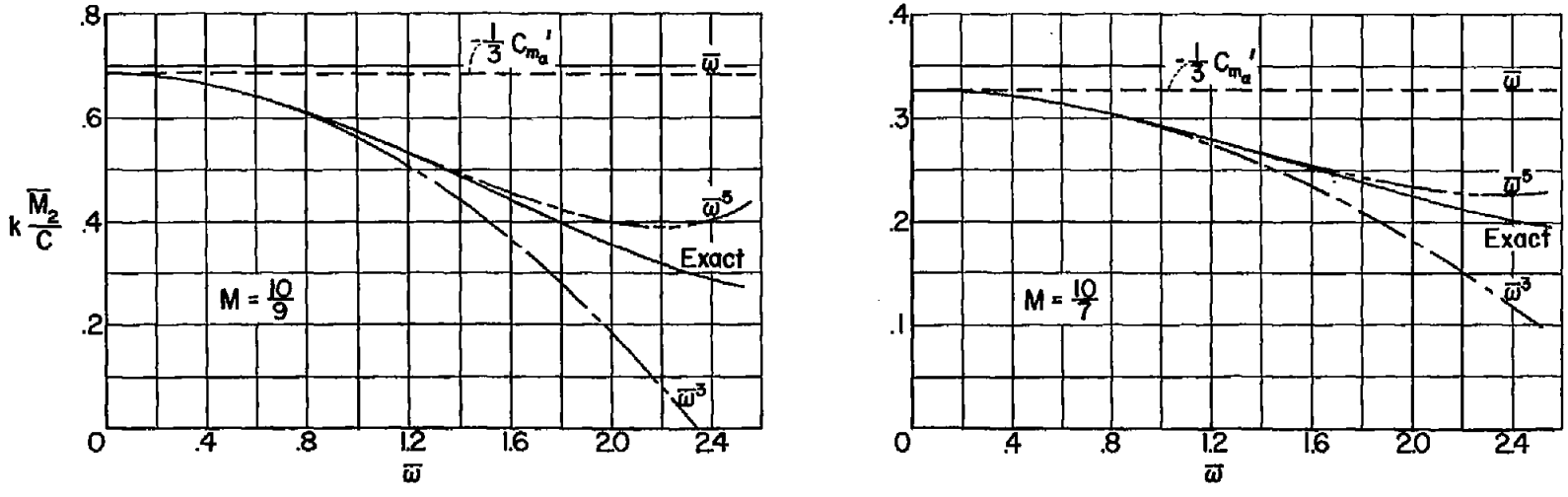

(f) Imaginary part of moment-curve slope associated with vertical translation of wing.

Figure 5.- Continued.

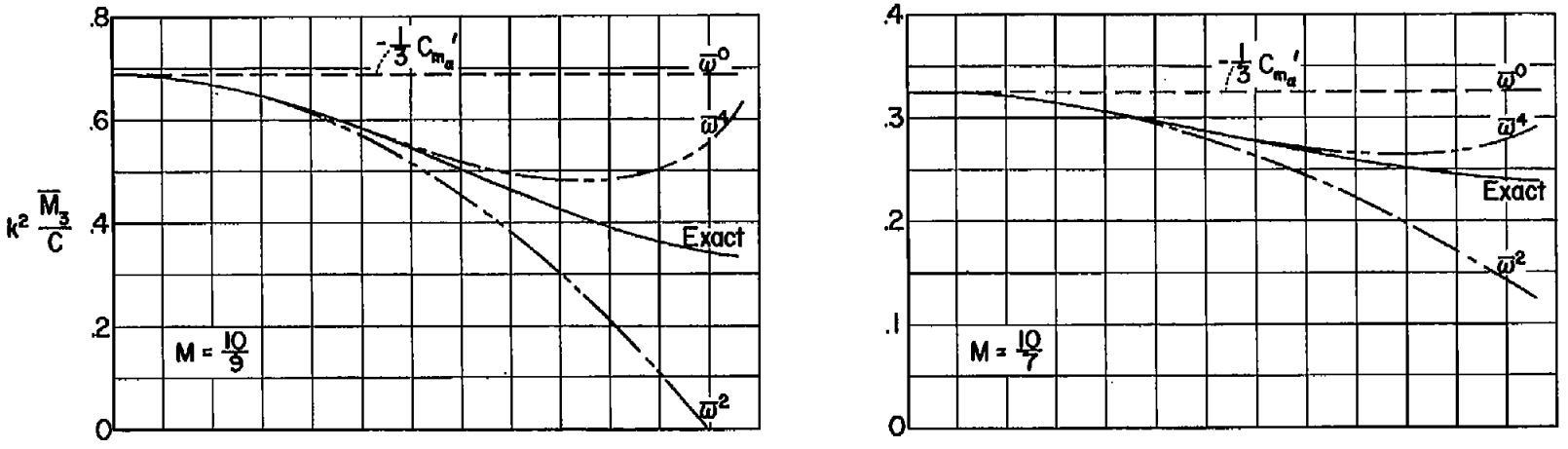

(g) Real part of moment-curve slope associated with pitching of wing.

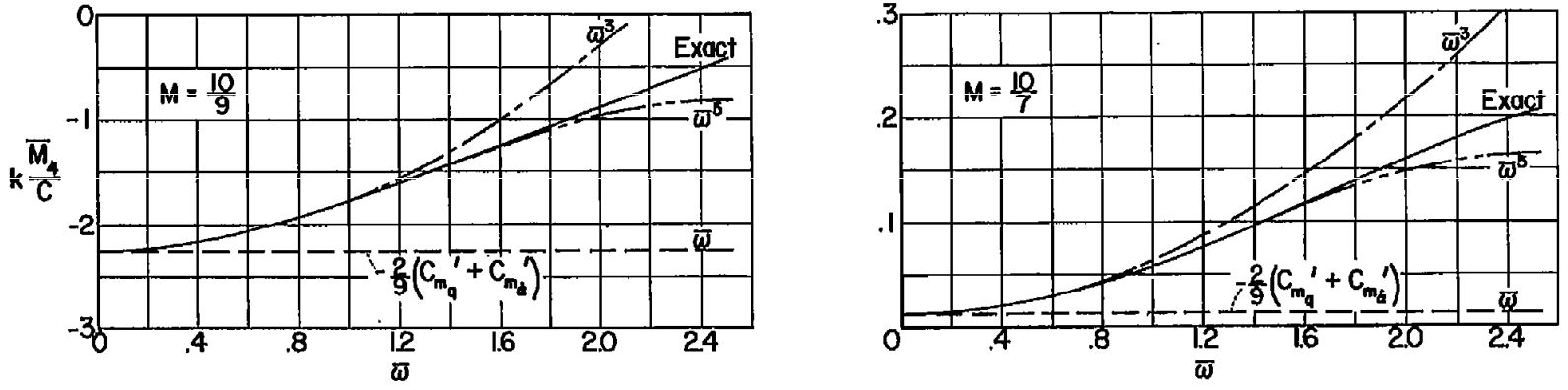

(h) Imaginary part of moment-curve slope associated with pitching of wing.

Figure 5.- Concluded.